

6509 **20.4 Solutions of Exercises of Chapter 9: Weak Focusing**
 6510 **Synchrotron**

6511 **9.1**

6512 **Construct Saturne I. Spin Resonances**

6513 A photo of Saturne I synchrotron can be found in Fig. 9.3. A schematic layout of
 6514 the ring and 90 deg cell is given in Fig. 9.23. This figure as well as Tab. 9.2 which
 6515 lists the parameters of the synchrotron, will be referred to in building the Saturne I
 6516 ring in the following.

6517 (a) A model of Saturne I synchrotron.

6518 DIPOLE is used to simulate the 90° cell dipole. It is necessary to have Fig. 20.55
 6519 at hand (in addition to the users' guide), when filling up the data list under DIPOLE.
 6520 Some comments regarding these data:

- 6521 • DIPOLE is defined in a cylindrical coordinate system.
- 6522 • The bending sector is 90 degrees, however the field region extent AT has to
 6523 encompass the fringe fields, at both ends of the 90 deg sector. A large 5 deg
 6524 extension is taken, for a total AT=100 deg which ensures absence of truncation of
 6525 the fringe fields at the AT sector boundaries, over the all radial excursion of the
 6526 beam.
- 6527 • RM is given the curvature radius value, $RM = B\rho/B = 0.274426548_{[Tm]}/0.03259493_{[T]} =$
 6528 8.4193 m, this makes magnet positioning and closed orbit checks easier (see be-
 6529 low). Note that the field and reference rigidity are, as for the simulation input
 6530 data, for 3.6 MeV, the injection energy, this is an arbitrary choice.
- 6531 • ACENT=50 deg is the reference azimuth, for the positioning of the entrance and
 6532 exit effective field boundaries (EFB). It is taken in the middle of the AT range, an
 6533 arbitrary choice.
- 6534 • The entrance radius in the AT sector is $RE = RM/\cos(AT - \omega^+) = RM/\cos(5^\circ)$,
 6535 with $\omega^+ = 45$ deg the positioning of the entrance EFB with respect to ACENT.
 6536 And similarly for the positioning of the exit reference frame, $RS = RM/\cos(AT -$
 6537 $(ACENT - \omega^-)) = RM/\cos(5^\circ)$ with $\omega^- = -45$ deg the positioning of the exit
 6538 EFB. Note that $\omega^+ - \omega^- = 90^\circ$, the value of the bend angle.
- 6539 • The entrance angle TE identifies with the extension to the 90 deg sector, namely,
 6540 TE=5 deg. And similarly for the positioning of exit frame, 5 deg downstream of
 6541 the exit EFB, thus TS=5 deg.

6542 In order to build the cell it is a good idea to proceed by steps:

6543 (i) first build a 90 deg deviation sector in the hard edge model (Tab. 20.46).
 6544 FAISCEAU located next to DIPOLE indicates that a trajectory entering DIPOLE
 6545 at radius R=RM, normally to the EFB (thus, $Y_0 = 0$ and $T_0 = 0$ in OBJET) exits
 6546 with Y=0 and T=0. Data validation at this stage can be performed by comparing
 6547 DIPOLE's transport matrix computed with MATRIX, and the theoretical expectation
 6548 (after Eq. ??, Sec. 19.5, numerical values truncated to 4th decimal)

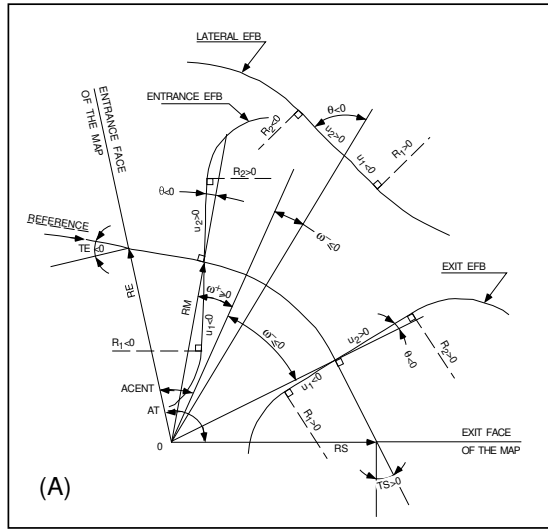


Fig. 20.55 This figure gives a representation of the data that define a dipole magnet, using DIPOLE [1]

$$T = \begin{pmatrix} \cos \sqrt{1-n}\alpha & \frac{\rho}{\sqrt{1-n}} \sin \sqrt{1-n}\alpha & 0 & 0 & 0 & \frac{\rho}{1-n} (1 - \cos \sqrt{1-n}\alpha) \\ -\frac{\sqrt{1-n}}{\rho} \sin \sqrt{1-n}\alpha & \cos \sqrt{1-n}\alpha & 0 & 0 & 0 & \frac{1}{\sqrt{1-n}} \sin \sqrt{1-n}\alpha \\ 0 & 0 & \cos \sqrt{n}\alpha & \frac{\rho}{\sqrt{n}} \sin \sqrt{n}\alpha & 0 & 0 \\ 0 & 0 & -\frac{\sqrt{n}}{\rho} \sin \sqrt{n}\alpha & \cos \sqrt{n}\alpha & 0 & 0 \\ \frac{1}{\sqrt{1-n}} \sin \sqrt{1-n}\alpha & \frac{\rho}{1-n} (1 - \cos \sqrt{1-n}\alpha) & 0 & 0 & 1 & \frac{\rho}{(1-n)^{3/2}} (\sqrt{1-n}\alpha - \sin \sqrt{1-n}\alpha) \\ 0 & 0 & 0 & 0 & 0 & 1 \end{pmatrix}$$

$$\begin{matrix} \alpha = \pi/2, \\ \rho = 8.4193 \\ n = 0.6 \\ \longrightarrow \end{matrix} \begin{pmatrix} 0.545794 & 11.15444 & 0 & 0 & 0 & 9.560222 \\ 0.062944 & 0.545794 & 0 & 0 & 0 & 1.324865 \\ 0 & 0 & 0.346711 & 10.19506 & 0 & 0 \\ 0 & 0 & -0.086295 & 0.346711 & 0 & 0 \\ 1.324865 & 9.560222 & 0 & 0 & 1 & 5.17640 \\ 0 & 0 & 0 & 0 & 0 & 1 \end{pmatrix} \quad (20.13)$$

6549 MATRIX computation outcomes from raytracing can be found for comparison in
6550 Tab. 20.47.

6551 It is leisable, at this point, to choose to add fringe fields. This is the case in
6552 Exercise 9.2, however the hard edge model will be carried on with, here.

6553 (ii) next, assemble a cell including this dipole with a pair of half-drifts at each
6554 ends, 2 m each (Fig. 9.23 and Tab. 20.48).

Table 20.46 Simulation input data file: a 45 degree sector bend in the hard edge model. The magnet is split into two identical halves, this is in order to allow access to particle coordinates at the center of the dipole, via FAISTORE or (here) FAISCEAU. The reference trajectory has equal entrance and exit position, and opposite sign angles. It coincides with the arc $R=RM$. MATRIX computes the transport matrix of the dipole (bottom of this Table), for comparison with the fringe field model, and possible comparison with matrix codes outcomes. This input data file is named SatI_DIP.inc and defines the Saturne I cell sequence segment S_SatI_DIP to E_SatI_DIP, for use with INCLUDE in subsequent exercises

```

File name: SatI_DIP.inc
Saturne I. Hard edge dipole model. Transport matrix.
'OBJET'
0.274426548e3                               ! Reference Brho: 3.6 MeV proton.
5                                             ! Create an 11 particle set, proper for MATRIX computation.
.001 .01 .001 .01 .001 .0001                ! Coordinate sampling.
0. 0. 0. 0. 0. 1. 'o'                       ! Reference trajectory: all initial coordinates nul, relative rigidity D=1.
1
'MARKER' S_SatI_DIP                          ! Cell dipole begins here.
'DIPOLE' upstream_half                       ! Analytical modeling of a dipole magnet.
0                                             ! IL=2 here, to log trajectory coordinates in zgoubi.plt, at integration steps.
45. 841.93                                   ! Field region angle=90; reference radius set to curvature radius value.
22.5 0.3259493638 -0.6 0. 0.               ! Reference angle ACENT set to AT/2; Bo field at RM; indices, all zero.
.0 0.                                         ! EFB 1 with fringe field extent.
4 .1455 2.2670 -.6395 1.1558 0. 0. 0.     ! Enge coefficients.
22.5 0. 1.E6 -1.E6 1.E6 1.E6               ! Angle to ACENT; face angle; face is straight.
.0 0.                                         ! EFB 2.
4 .1455 2.2670 -.6395 1.1558 0. 0. 0.     ! Enge coefficients.
-22.5 0. 1.E6 -1.E6 1.E6 1.E6             ! Angle to ACENT; face angle; face is straight.
0. 0.                                         ! EFB 3. Unused.
0. 0. 0. 0. 0. 0. 0. 0. 0. 0. 0.         ! EFB 3. Unused.
0. 0. 1.E6 -1.E6 1.E6 1.E6 0.              ! Degree of interpolation polynomial; flying grid sizing.
2 1                                           ! Integration step size. It can be large in uniform field.
2. 841.93 0. 841.93 0.                     ! Positioning of entrance and exit frames.
'MARKER' half-dipole !.plt                  ! Uncomment LABEL_2='! .plt' (may go with IL=2 under DIPOLE) to
! log particle data in zgoubi.plt.
'FAISCEAU' ! Provides local coordinates, and ellipse parameters, at center of Saturne I dipole.
'DIPOLE' downstream_half                   ! Analytical modeling of a dipole magnet.
0                                             ! IL=2 here, to log trajectory coordinates in zgoubi.plt, at integration steps.
45. 841.93                                   ! Field region angle=90; reference radius set to curvature radius value.
22.5 0.3259493638 -0.6 0. 0.               ! Reference angle ACENT set to AT/2; Bo field at RM; indices, all zero.
.0 0.                                         ! EFB 1 with fringe field extent.
4 .1455 2.2670 -.6395 1.1558 0. 0. 0.     ! Enge coefficients.
22.5 0. 1.E6 -1.E6 1.E6 1.E6               ! Angle to ACENT; face angle; face is straight.
.0 0.                                         ! EFB 2.
4 .1455 2.2670 -.6395 1.1558 0. 0. 0.     ! Enge coefficients.
-22.5 0. 1.E6 -1.E6 1.E6 1.E6             ! Angle to ACENT; face angle; face is straight.
0. 0.                                         ! EFB 3. Unused.
0. 0. 0. 0. 0. 0. 0. 0. 0. 0. 0.         ! EFB 3. Unused.
0. 0. 1.E6 -1.E6 1.E6 1.E6 0.              ! Degree of interpolation polynomial; flying grid sizing.
2 1                                           ! Integration step size. It can be large in uniform field.
2. 841.93 0. 841.93 0.                     ! Positioning of entrance and exit frames.
'MARKER' E_SatI_DIP                          ! Cell dipole ends here.
'FAISCEAU' ! Local particle coordinates.
'MATRIX' ! Compute transport matrix, from trajectory coordinates.
1 0
'END'

```

Table 20.47 Outcomes of the simulation file of Tab. 20.46

An excerpt from *zgoubi.res*. Coordinates of the first particle (the reference trajectory) and its path length under FAISCEAU, at OBJET on the left hand side below, locally on the right hand side:

```

3 Keyword, label(s) : FAISCEAU                                     IPASS= 1
                                     TRACE DU FAISCEAU
                                     (follows element # 2)
                                     11 TRAJECTOIRES
OBJET
      D      Y(cm)    T(mr)    Z(cm)    P(mr)    S(cm)    D-1    Y(cm)    T(mr)    Z(cm)    P(mr)    S(cm)
0 1 1.0000  0.000  0.000  0.000  0.000  0.0000  0.0000  0.000  0.000  0.000  1.322501E+03
    
```

Transport matrix of Saturne I90 degree sector bend, in the hard edge model, two difference cases of integration step size, namely, 4 cm and 1 m (an excerpt of MATRIX computation, from *zgoubi.res*). It can be checked against matrix transport expectations. The "first order symplectic conditions" are very small in the 4 cm step size case, which is an indication of accurate numerical integration of the trajectories across DIPOLE; the reference trajectory (first one) exits better aligned (reference coordinates, before change of frame for MATRIX computation, are closer to zero):

- Case of 4 cm step size:

```

4 Keyword, label(s) : MATRIX                                     IPASS= 1
Reference, before change of frame (particle # 1 - D-1,Y,T,Z,s,time) :
0.00000000E+00  4.53054326E-07  6.27843350E-07  0.00000000E+00  0.00000000E+00  1.32250055E+03  4.41138700E-02

      TRANSFER MATRIX ORDRE 1 (MKSA units)
      0.545795      11.1544      0.000000      0.000000      0.000000      9.56022
      -6.294423E-02  0.545795      0.000000      0.000000      0.000000      1.32487
      0.000000      0.000000      0.346711      10.1951      0.000000      0.000000
      0.000000      0.000000      -8.629576E-02  0.346711      0.000000      0.000000
      1.32487      9.56022      0.000000      0.000000      1.000000      5.17640
      0.000000      0.000000      0.000000      0.000000      0.000000      1.00000

      DetY-1 = 0.0000000278,      DetZ-1 = 0.0000000045
      R12=0 at -20.44 m,      R34=0 at -29.41 m
First order symplectic conditions (expected values = 0) :
2.7767E-08  4.4762E-09  0.000  0.000  0.000  0.000
    
```

- Case of 1 m step size:

```

4 Keyword, label(s) : MATRIX                                     IPASS= 1
Reference, before change of frame (particle # 1 - D-1,Y,T,Z,s,time) :
0.00000000E+00  -7.54923113E-03  -1.08904867E-02  0.00000000E+00  0.00000000E+00  1.32249873E+03  4.41138091E-02

      TRANSFER MATRIX ORDRE 1 (MKSA units)
      0.545757      11.1567      0.000000      0.000000      0.000000      9.56154
      -6.295274E-02  0.546125      0.000000      0.000000      0.000000      1.32517
      0.000000      0.000000      0.346697      10.1954      0.000000      0.000000
      0.000000      0.000000      -8.629900E-02  0.346750      0.000000      0.000000
      1.32486      9.56148      0.000000      0.000000      1.000000      5.17692
      0.000000      0.000000      0.000000      0.000000      0.000000      1.00000

      DetY-1 = 0.0003978566,      DetZ-1 = 0.0000685588
      R12=0 at -20.43 m,      R34=0 at -29.40 m
First order symplectic conditions (expected values = 0) :
3.9786E-04  6.8559E-05  0.000  0.000  0.000  0.000
    
```

Table 20.48 Simulation input data file: Saturne I cell, obtained by assembling DIPOLE taken from Tab. 20.46 together with two half-drifts. This input data file is named SatI_cell.inc and defines the Saturne I cell sequence segment S_SatI_cell to E_SatI_cell, for possible use in INCLUDE statements in subsequent exercises

```

File name: SatI_cell.inc.
! Saturne I, one cell of the 4-period ring.
'MARKER' SatICellMATRIX_S ! Just for edition purposes.
'OBJET'
0.274426548e3 ! Reference Brho: 3.6 MeV proton.
5 ! Create an 11 particle set, proper for MATRIX computation.
.001 .01 .001 .01 .001 .0001 ! Coordinate sampling.
0. 0. 0. 0. 0. 1. ! Reference trajectory: all initial coordinates nul, relative rigidity D=1.
1

'MARKER' S_SatI_cell
'DRIFT' half_drift
200.
'INCLUDE'
1
./SatI_DIP.inc[S_SatI_DIP:E_SatI_DIP]
'DRIFT' half_drift
200.
'MARKER' E_SatI_cell
'FAISCEAU' ! Local particle coordinates.
'TWISS'
2 1. 1.
'MARKER' SatICellMATRIX_E ! Just for edition purposes.
'END'

```

6555 *Lattice parameters*

6556 The TWISS command down the sequence (Tab. 20.48) produces the periodic beam matrix results shown in Tab. 20.49

Table 20.49 Results obtained running the simulation input data file of Tab. 20.48, Saturne I cell - an excerpt from zgoubi.res

```

14 Keyword, label(s) : TWISS                                     IPASS= 4
Reference, before change of frame (particle # 1 - D-1,Y,T,Z,s,time) :
0.00000000E+00 6.02895730E-07 6.54169939E-07 0.00000000E+00 0.00000000E+00 1.72250055E+03 6.57784696E-01

Beam matrix (beta/-alpha/-alpha/gamma) and periodic dispersion (MKSA units)
14.418595 0.000000 0.000000 0.000000 0.000000 21.048250
0.000000 0.069355 0.000000 0.000000 0.000000 0.000000
0.000000 0.000000 11.411041 0.000000 0.000000 -0.000000
0.000000 0.000000 0.000000 0.087634 0.000000 0.000000
0.000000 0.000000 0.000000 0.000000 0.000000 0.000000
0.000000 0.000000 0.000000 0.000000 0.000000 0.000000

          Betatron tunes (Q1 Q2 modes)
NU_Y = 0.18103144          NU_Z = 0.22214599

          dL/L / dp/p = 1.9194487
(dp = 0.000000E+00  L(0) = 1.72250E+03 cm,  L(0)-L(-dp) = 3.30606E-01 cm,  L(0)-L(+dp) = -3.30645E-01 cm)

          Transition gamma = 7.21791469E-01

          Chromaticities :
dNu_y / dp/p = -0.60221729          dNu_z / dp/p = 0.38005442

```

6557

6558 The TWISS command also produces a zgoubi.TWISS.out file which details the
6559 optical functions along the sequence (at the downstream end of the optical elements.
6560 The header of that file details the optical parameters of the structure (Tab. 20.50).

Table 20.50 An excerpt of zgoubi.TWISS.out file resulting from the execution of the Saturne I cell simulation input data file of Tab. 20.48. Note that the ring (4-period) wave numbers are 4 times the cell values Q1, Q2 displayed here. Optical functions (betatron function and derivative, orbit, phase advance, etc.) along the optical sequence are listed as part of zgoubi.TWISS.out following the header. The top part and last line of that listing are given below

```

@ LENGTH          %le  17.22500552
@ ALFA            %le  1.919448707
@ ORBIT5          %le
@ GAMMATR        %le  0.7217914685
@ Q1              %le  0.1810314404 [fractional]
@ Q2              %le  0.2221459901 [fractional]
@ DQ1             %le  -0.6022172911
@ DQ2            %le  0.3800544183
@ DXMAX          %le  2.10586311E+01 @ DXMIN          %le  2.10482503E+01
@ DYMAX          %le  0.00000000E+00 @ DYMIN          %le  0.00000000E+00
@ XCOMAX        %le  2.10528899E-01 @ XCOMIN        %le  0.00000000E+00
@ YCOMAX        %le  0.00000000E+00 @ YCOMIN        %le  0.00000000E+00
@ BETMAX        %le  1.57006971E+01 @ BETXMIN        %le  1.44132839E+01
@ BETYMAX        %le  1.30884296E+01 @ BETYMIN        %le  1.14110171E+01
@ XCORMS        %le  6.05227342E-04
@ YCORMS        %le  0. not computed
@ DXRMS         %le  2.98427468E-03
@ DYRMS         %le  0.00000000E+00

```

Top and bottom four lines (truncated) of zgoubi.TWISS.out optical functions listing, including the periodic β_x , β_y (β_Y , β_Z in zgoubi notations) and D_x (η_Y in zgoubi notations) values at cell ends:

```

# alfx          btx          alfy          bty          alfl          btl          Dx          Dxp
3.1789380E-009  1.4426805E+001  -8.1670406E-009  1.1411067E+001  0.0000000E+000  0.0000000E+000  2.1058631E+001  1.1261478E-003
1.3369744E-008  1.4426805E+001  -1.7451004E-009  1.1411067E+001  0.0000000E+000  0.0000000E+000  2.1048250E+001  1.6725930E-009
1.3369744E-008  1.4426805E+001  -1.7451004E-009  1.1411067E+001  0.0000000E+000  0.0000000E+000  2.1048250E+001  1.6725930E-009
-1.3863082E-001  1.4704066E+001  -1.7526845E-001  1.1761604E+001  0.0000000E+000  0.0000000E+000  2.1048250E+001  1.6725930E-009
.....
1.3919473E-001  1.4692541E+001  1.7526999E-001  1.1761559E+001  0.0000000E+000  0.0000000E+000  2.1048250E+001  1.6725925E-009
1.3919473E-001  1.4692541E+001  1.7526999E-001  1.1761559E+001  0.0000000E+000  0.0000000E+000  2.1048250E+001  1.6725925E-009
4.3382070E-004  1.4413284E+001  7.7156422E-007  1.1411017E+001  0.0000000E+000  0.0000000E+000  2.1048250E+001  1.6725925E-009
4.3382070E-004  1.4413284E+001  7.7156422E-007  1.1411017E+001  0.0000000E+000  0.0000000E+000  2.1048250E+001  1.6725925E-009

```

6561 *Tune scan*

6562 A simulation is given in Tab. 20.51, derived from Tab. 20.48: TWISS has been
6563 replaced by MATRIX, a REBELOTE do loop repeatedly changes n . A plot of the
6564 scan is given in Fig. 20.56, some detailed values are given in Tab. 20.52.

Table 20.51 Simulation input data file: tune scan, using REBELOTE to repeatedly change n . Beam matrix and wave numbers are computed by MATRIX, from the coordinates of the 11 particle sample generated by OBJET[KOBJ=5]

```
Saturne I, tune scan.
'MARKER' SatI_Qscan_S ! Just for edition purposes.
'OBJET'
0.274426548e3 ! Reference Brho: 3.6 MeV proton.
5 ! Create an 11 particle set, proper for MATRIX computation.
.001 .01 .001 .01 .001 .0001 ! Coordinate sampling.
0. 0. 0. 0. 0. 1. ! Reference trajectory: all initial coordinates nul, relative rigidity D=1.
1

'MARKER' S_SatI_cell
'DRIFT' half_drift
200.
'INCLUDE'
1
./SatI_DIP.inc[S_SatI_DIP:E_SatI_DIP]
'DRIFT' half_drift
200.
'MARKER' E_SatI_cell
'FAISCEAU' ! Local particle coordinates.
'MATRIX'
1 11 PRINT ! Comoute a 10+4 period transport matrix, and tunes. Save outcomes to zgoubi.MATRIX.out.

'REBELOTE' ! A do loop: repeat the section above commencing at the top of the file,
10 1.1 0 1 ! 10 times.
1
DIPOLE 6 -0.757:-0.5 ! Change the value of parameter 30 (namely, n) in DIPOLE (prior to repeating).
! in any DIPOLE in the sequence.

'SYSTEM'
1
gnuplot <./gnuplot_MATRIX_Qxy.gnu ! Plot tunes vs index.
'MARKER' SatI_Qscan_E ! Just for edition purposes.
'END'
```

gnuplot script to obtain Fig. 20.56:

```
# ./gnuplot_MATRIX_Qxy.gnu
set xlabel "index n"; set ylabel "{/Symbol n}_x, ({/Symbol n}_x^2+{/Symbol n}_y^2)^{1/2}"
set ylabel "{/Symbol n}_y"; set xtics; set ytics nomirror; set y2tics nomirror; ncell=4
set key t 1; set key maxrow 2; set yrange [:1.3]; set y2range [:1.06]
n1 = -0.757; dn=(.757-.5)/10.; R=10.9658; rho=8.4193
plot \
"zgoubi.MATRIX.out" u (n1+($61-1)*dn): \
($61>1? $56 *ncell :1/0) w p pt 5 lt 1 lw .5 lc rgb "red" tit "{/Symbol n}_x " , \
"zgoubi.MATRIX.out" u (n1+($61-1)*dn):($61>1? sqrt((1+(n1+($61-1)*dn))*R/rho): \
1/0) w l lt 1 lc rgb "red" tit "theor. " , \
"zgoubi.MATRIX.out" u (n1+($61-1)*dn): \
($61>1? $57 *ncell :1/0) axes xly2 w p pt 6 lt 3 lw .5 lc rgb "blue" tit "{/Symbol n}_y " , \
"zgoubi.MATRIX.out" u (n1+($61-1)*dn): \
($61>1? sqrt((-n1+($61-1)*dn))*R/rho):1/0) axes xzy2 w l lt 3 lc rgb "blue" tit "theor. " , \
"zgoubi.MATRIX.out" u (n1+($61-1)*dn): \
($61>1? sqrt($56**2+$57**2) *ncell :1/0) w p pt 7 lt 1 lc rgb "black" tit "({/Symbol n}_x^2+{/Symbol n}_y^2)^{1/2}" , \
"zgoubi.MATRIX.out" u (n1+($61-1)*dn):($61>1? sqrt(R/rho):1/0) w l lt 1 lc rgb "black" tit "theor. "
pause 1
```

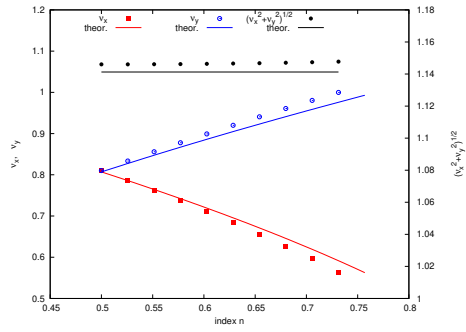



Fig. 20.56 A scan of the wave numbers, and of $\sqrt{v_Y^2 + v_Z^2} \approx \sqrt{R/\rho_0} = 1.141$, in Saturne I for $0.5 \leq n \leq 0.757$

Table 20.52 Dependence of wave numbers on index n , from numerical raytracing (columns denoted “ray-tr.”) and from theory

n	v_Y		v_Z	
	ray-tr.	$\sqrt{(1-n)\frac{R}{\rho_0}}$	ray-tr.	$\sqrt{n\frac{R}{\rho_0}}$
0.5	0.810353	0.806987	0.810353	0.806987
0.6	0.724125	0.721791	0.888583	0.884010
0.7	0.626561	0.625089	0.960806	0.954840
0.757	0.563635	0.562580	0.999804	0.992955

6565 (b) Betatron functions of Saturne I cell.

6566 Among the various ways to produce the betatron functions along the sequence
6567 (and throughout the DIPOLES), here are two possibilities, based on the storage of
6568 particle coordinates in zgoubi.plt during stepwise raytracing:

- 6569 1. a direct way consists in using OBJET[KOBJ=5.1] and transport the 11-particle
6570 set so obtained across the sequence. Then, betaFromPlt from zgoubi toolbox [2]
6571 can be used to compute the transport matrix, step by step across the sequence,
6572 from the coordinate values logged in zgoubi.plt during the stepwise integration;
- 6573 2. an indirect way consists in launching a few particles on a common invariant (hor-
6574 izontal and/or vertical) and subsequently plot the s-dependent quantities $\hat{Y}^2(s)/\epsilon_Y$
6575 and/or $\hat{Z}^2(s)/\epsilon_Z$. The maximum value of the latter, a function of the distance s,
6576 is the betatron function along the sequence, $\beta_{Y,Z}(s)$.

6577 The second method is used here (this is an arbitrary choice. Exercises may be
6578 found in the various Chapters, that use the first method and may be referred to, if
6579 desired).

The input data file to derive the betatron function following method (2) above is given in Tab. 20.53. The initial ellipse parameters (under OBJET) are the periodic values, namely, $\alpha_Y = \alpha_Z = 0$, $\beta_Y = 14.426$ m, $\beta_Z = 11.411$ m, they are a sub-product of the TWISS procedure performed in (a), to be found in zgoubi.TWISS.out (Tab. 20.50). The resulting envelopes and their squared value are shown in Fig. 20.57. Note that this raytracing also provides the coordinates of the 60 particles on their common upright invariant

$$x^2/\beta_x + \beta_x x'^2 = \epsilon_x/\pi$$

6580 at start and at the end of the cell (with x standing for either Y or Z, and $\epsilon_{Y,Z}/\pi =$
6581 10^{-4} , here). This allows checking that the initial ellipse parameters (under OBJET,
6582 Tab. 20.53) are effectively periodic values, and that the raytracing went correctly,
6583 namely by observing that the initial and final ellipses do superimpose (Fig. 20.58).

Table 20.53 Simulation input data file: raytrace 60 particles across Saturne I cell to generate beam envelopes. Store particle data in zgoubi.plt, along DRIFTS and DIPOLES. The INCLUDE file and segments are defined in Tab. 20.48

```

SatI envelopes.
'OBJET'
0.274426548e3                               ! Reference Brho: 3.6 MeV proton.
8                                               ! Create a set of 60 particles evenly distributed on the same invariant;
1 60 1   ! case of 60 particles on a vertical invariant; use 60 1 1 instead for horizontal invariant.
0. 0. 0. 0. 0. 1.
0. 14.426 1e-4
0. 11.411 1e-4
0. 1. 0.

'FAISTORE'                                     ! This logs the coordinates of the particle to zgoubi.fai,
zgoubi.fai  S_SatI_cell  E_SatI_cell          ! at the two LABELIs as indicated.
1

'MARKER'  S_SatI_cell                          ! Saturne I cell begins here.
'DRIFT'  half_Drift                            ! Option 'split' divides the drift in 10 pieces,
200. split 10 2                               ! 'IL=2' causes log of particle data to zgoubi.plt.

'INCLUDE'
1
./SatI_DIP.inc[S_SatI_DIP:E_SatI_DIP]

'DRIFT'  half_Drift                            ! Option 'split' divides the drift in 10 pieces,
200. split 10 2                               ! 'IL=2' causes log of particle data to zgoubi.plt.

'MARKER'  E_SatI_cell                          ! Saturne I cell ends here.
'FAISCEAU'
'END'

```

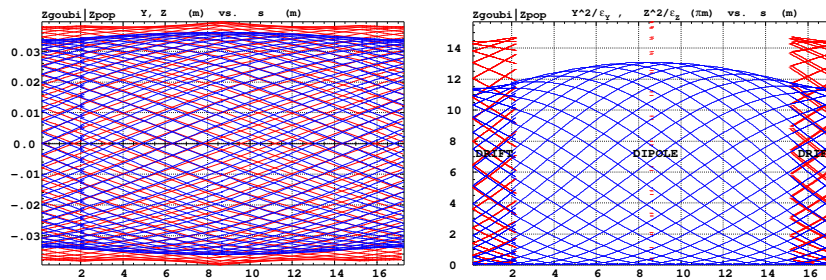


Fig. 20.57 Left: horizontal and vertical envelopes as generated by plotting the coordinates $Y(s)$ (greater excursion, red, along the drifts and at dipole center) or $Z(s)$ (smaller excursion, blue) across the Saturne I cell, of 60 particles evenly distributed on a common $10^{-4} \pi \mu\text{m}$ invariant, either horizontal or vertical (while the other invariant is zero). Right: a plot of $Y^2(s)/\epsilon_Y$ and $Z^2(s)/\epsilon_Z$: the extrema identify with $\beta_Y(s)$ and $\beta_Z(s)$, respectively. The extrema extremorum values are $\hat{\beta}_Y = 14.4 \text{ m}$ and $\hat{\beta}_Z = 15.7 \text{ m}$, respectively. These plots are obtained using zpop, which reads stepwise particle data from zgoubi.plt

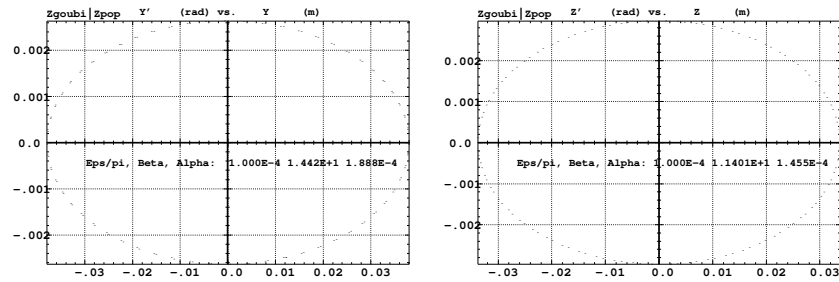


Fig. 20.58 Sixty particles evenly distributed on a common periodic invariant (of value either $\epsilon_Y = 10^{-4} \pi \mu\text{m}$ and $\epsilon_Z = 0$, left plot, or the reverse, right plot) have been tracked from start to end of the cell. These periodic invariants are defined assuming the periodic ellipse parameters determined from prior TWISS, given in Tab. 20.50; values resulting from an *rms* match of the coordinates are given in the figure, and do agree with those TWISS data. The figure shows the good superposition of the start and end invariants (the start and end *rms* match ellipse parameters show negligible difference), which confirms the correct value of the periodic ellipse parameters, namely, left graph: horizontal phase space at start (crosses) and end (dots) of the cell; right graph: vertical phase space at start (crosses) and end (dots) of the cell

6584 *Dispersion function*

6585 Raytracing off-momentum particles on their chromatic closed orbit provides the
 6586 periodic dispersion function. In order to do so, the input data file of Tab. 20.53 can
 6587 be used, it just requires changing OBJET to the following:

```
6588 'OBJET'
6589 0.274426548e3 ! Reference Brho: 3.6 MeV proton.
6590 2 ! Create particles individually.
6591 3 1 ! Three particles.
6592 +.21056 0. 0. 0. 1.0001 'p' ! Chromatic orbit coordinates Y0 and T0 for D=1.001 relative rigidity.
6593 0. 0. 0. 0. 1. 'o' ! On-momentum orbit.
6594 -.21056 0. 0. 0. 0.9999 'm' ! Chromatic orbit coordinates Y0 and T0 for D=0.999 relative rigidity.
6595 1 1 1
```

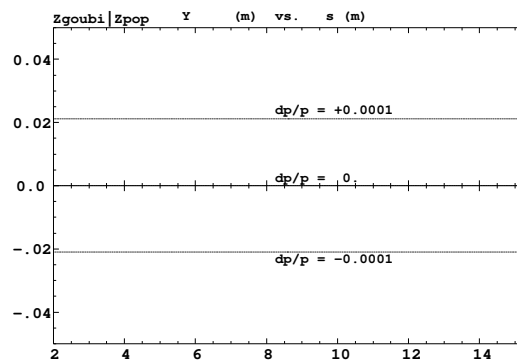
6596 The position and angle of the chromatic particles, which are offset by $\Delta p/p =$
 6597 $\pm 10^{-4}$, are drawn from the value of the periodic dispersion $\eta_Y = 21.05$ m and
 6598 its derivative $\eta'_Y \approx 0$ (Tab. 20.50), namely, $Y_0 = \eta_Y \Delta p/p = \pm 0.2105$ cm and
 6599 $T_0 = \eta'_Y \Delta p/p = 0$.

6600 Running Tab. 20.53 simulation file with this new OBJET produces the following
 6601 coordinates at FAISCEAU, located at the end of the sequence (an excerpt from
 6602 zgoubi.res):

```
6603 13 Keyword, label(s) : FAISCEAU IPASS= 1
6604 TRACE DU FAISCEAU
6605 (follows element # 12)
6606 3 TRAJECTOIRES
6607 OBJET FAISCEAU
6608 D Y(cm) T(mr) Z(cm) P(mr) S(cm) D-1 Y(cm) T(mr) Z(cm) P(mr) S(cm)
6609 p 1 1.0001 0.211 0.000 0.000 0.000 0.0000 0.0001 0.211 0.000 0.000 0.000 1.722831E+03 1
6610 o 1 1.0000 0.000 0.000 0.000 0.000 0.0000 0.0000 0.000 0.000 0.000 0.000 1.722501E+03 2
6611 m 1 0.9999 -0.211 0.000 0.000 0.000 0.0000 -0.0001 -0.210 0.000 0.000 0.000 1.722170E+03 3
```

6612 The local coordinates Y, T (under FAISCEAU, right hand side) and initial co-
 6613 ordinates Y_0, T_0 (under OBJET, left hand side) are identical (to better than $5 \mu\text{m}$,
 6614 $0.5 \mu\text{rad}$ accuracy, respectively - zgoubi.fai can be consulted for greater precision on
 6615 these values), confirming the periodicity of these chromatic trajectories. Figure 20.59
 6616 shows the particle trajectories through the cell DIPOLE, they appear to be at constant
 6617 radius as expected.

Fig. 20.59 A plot of the radial excursion, across DIPOLE body (namely, AT=90° extent, (Tab. 20.48), of an on-momentum particle (its radial position along the dipole body is $R_0 \approx 8.4193$ m, corresponding to $Y=0$ in this graph) and two particles at respectively $dp/p = \pm 10^{-3}$. A graph obtained using zpop, which reads stepwise particle data from zgoubi.plt; menu 7; 1/1 to open zgoubi.plt; 2/[6,2] to select Y versus distance; 7 to plot



6618 (c) Some verifications regarding the model.

6619 The field along large excursion orbits can be logged in zgoubi.plt, using option
6620 IL=2 (or 20, or 200, etc. for printout every 10, or 100, etc. integration step) under
6621 DIPOLE.

6622 The simulation file of Tab. 20.53 is used to raytrace five particles, with OBJET
6623 changed to the following:

```

6624 'OBJET'
6625 0.274426548e3 ! Reference Brho: 3.6 MeV proton.
6626 2 ! Create particles individually,
6627 5 1 ! five particles.
6628 +0.21056 0. 0. 0. 1.01 'p' ! Chromatic orbit coordinates for D=1.01 relative rigidity.
6629 0. 0. 0. 0. 1. '0' ! On-momentum closed orbit.
6630 -0.21056 0. 0. 0. 0.99 'm' ! Chromatic orbit coordinates for D=0.99 relative rigidity.
6631 0. 0. 5. 0. 1. 'm' ! Initial vertical excursion is Z0= 5 cm off-mid-plane.
6632 0. 0. 20. 0. 1. 'm' ! Initial vertical excursion is Z0=20 cm off-mid-plane.
6633 1 1 1 1 1

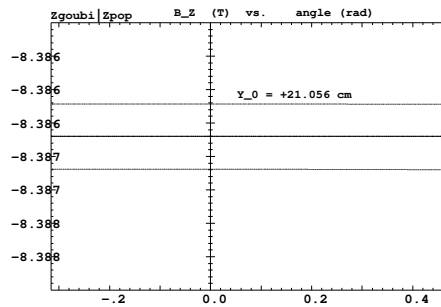
```

6634 Apart from the on-momentum particle (2nd in the list) this OBJET defines two
6635 particles on $\Delta p/p = \pm 1\%$ chromatic orbit (1st and 3rd in the list), this is an excursion
6636 of a few tens of centimeters, large as requested, as $\Delta x \approx 38 \times dp/p$. OBJET also
6637 defines 2 particles launched into the cell at respectively $Z_0 = 5$ cm and $Z_0 = 20$ cm.

6638 The magnetic field as a function of the azimuthal angle in DIPOLE frame, along
6639 these trajectories across the upstream DIPOLE of the cell, is shown in Fig. 20.60.
6640 The field curves for the first four trajectories essentially superimpose except for the
6641 fringe field regions (Fig. 20.60), due to the wedge angles. This behaves as expected.
6642 Detail inspection is possible, from the detailed particle coordinate and field data in
6643 zgoubi.plt - this is out of the scope of the present question.

6644 The field along the 5th particle trajectory features overshoots (Fig. 20.60), this
6645 is due to the very large vertical excursion ($Z \approx 20$ cm in the entrance fringe field
6646 region). It looks reasonable, however it may be an artifact in the case that the high
6647 order derivatives of the field in that region are large, resulting from the truncated
Taylor series method used for off mid-plane field extrapolation [1, Sec. 1.3.3].

Fig. 20.60 Magnetic field along 5 different trajectories across the upstream DIPOLE, including four large horizontal and vertical excursion cases



6649 (d) Sinusoidal approximation of the betatron motion.

The approximation

$$y(\theta) = A \cos(\nu_Z \theta + \phi)$$

6650 is checked here considering the vertical motion (considering the horizontal motion
6651 leads to similar conclusions). The value of the various parameters in that expression
6652 are determined as follows:

- the particle raytraced for comparison is launched with an initial excursion $Z_0(\theta = 0) = 5 \text{ cm}$ (4th particle in OBJET, above). At the launch point (middle of the drift) the beam ellipse is upright (Fig. 20.58), whereas phase space motion is clockwise, thus take

$$A = 5 \text{ cm} \quad \text{and} \quad \phi = \pi/2$$

- the vertical betatron of the 4-cell ring tune is (Tab. 20.50)

$$\nu_Z = 4 \times 0.222146 = 0.888284$$

- $\theta = s/R$ and $R = \oint ds/2\pi$ with (Tab. 20.50)

$$2\pi R = \text{circumference} = 2\pi \times 10.9658 = 68.9 \text{ m}$$

6653 The comparison with a trajectory obtained from raytracing is given in Fig. 20.61
6654 and confirms the validity of the sinusoidal approximation.

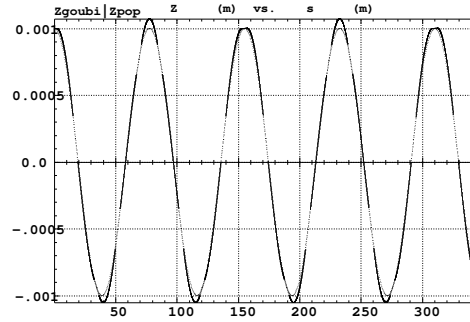


Fig. 20.61 Vertical betatron motion, five turns around Saturne I ring, from raytracing (modulated oscillation), and sine approximation, superimposed

6655 (e) An acceleration cycle. Symplecticity checks.

Eleven particles are launched for a 30,000 turn tracking at a rate of

$$\Delta W = q\hat{V} \cos \phi_s = 200 \times \sin 150^\circ = 100 \text{ keV/turn}$$

6656 ($E : 3.6 \rightarrow 3.0036 \text{ GeV}$), all evenly distributed on the same initial vertical invariant

$$Z^2/\beta_Z + \beta_Z Z'^2 = \epsilon_Z/\pi \quad (20.14)$$

6657 with $\epsilon_Z/\pi = 10^{-4} \text{ m}$, or, normalized, $\beta\gamma\epsilon_Z/\pi = 0.08768 \times 10^{-4} \text{ m}$.

The simulation file is given in Tab. 20.54. CAVITE[IOPT=3] is used, it provides an RF phase independent boost

$$\Delta W = q\hat{V} \sin \phi_s$$

6658 as including synchrotron motion is not necessary here, even better, this ensures
 6659 constant depolarizing resonance crossing speed, so precluding any possibility of
 6660 multiple crossing (it can be referred to [3] regarding that effect).

Table 20.54 Simulation input data file: track 11 particles launched on the same vertical invariant, with quasi-zero horizontal invariant. The INCLUDE adds the Saturne I cell four times, the latter is defined in Tab. 20.48 and Fig. 9.23

```

Saturne I ring. Polarization landscape.
'MARKER' SatIPolarLand_S ! Just for edition purposes.
'OBJET'
0.274426548e3 ! Reference Brho: 3.6 MeV proton.
8 ! Create a set of 60 particles evenly distributed on the same invariant;
1 11 1 ! case of 60 particles on a vertical invariant; use 60 1 1 instead for horizontal invariant.
0. 0. 0. 0. 0. 1.
0. 14.426 1e-4 ! Periodic optical functions and invariant value, horizontal and
0. 11.411 1e-4 ! vertical.
0. 1. 0. ! No momentum spread.

!'MCOBJET' ! Commented.
11.03527036749193e3 ! Reference Brho: 50 MeV proton.
13 ! Create an 11 particle set, proper for MATRIX computation.
!200
!2 2 2 2 2 2
!0. 0. 0. 0. 0. 1.
!0. 14.426 25e-6 3 ! Periodic alpha_Y, beta_Y, and invariant value;
!0. 11.411 10e-6 3 ! Periodic alpha_Z, beta_Z, and invariant value.
!0. 1. 1.e-8 3
!123456 234567 345678

'PARTICUL'
PROTON ! Necessary data in order to allow (i) spin trackingand, and (ii) acceleration.
'SPNTRK' ! Switch on spin tracking,
3 ! all initial spins vertical.
'FAISCEAU'
'FAISTORE'
b_polarLand.fai ! Log particle data in b_polarLand.fai, turn-by-turn; "b_" imposes
7 ! binary write, which results in faster i/o.

'SCALING'
1 1
DIPOLE
-1 ! Causes field increase in DIPOLE, in correlation to particle
1. ! rigidity increase by CAVITE.
1

! 4 cells follow.
'INCLUDE'
1
4* ./SatI_cell.inc[S_SatI_cell:E_SatI_cell]

'CAVITE'
3
0 0
200e3 0.523598775598 ! Acceleration rate is 200*0.5=100keV/turn.
! 20e3 0.523598775598 ! Commented: an acceleration rate of 20*0.5=10keV/turn.

'REBELOTE'
30000 0.3 99 ! Case of 100 keV/turn: ~30,000 turns from 3.6 MeV to 3 GeV.
! 30000 0.3 99 ! Commented: case of 10 keV/turn: ~300,000 turns from 3.6 MeV to 3 GeV.

'FAISCEAU'
'MARKER' SatIPolarLand_E ! Just for edition purposes.
'SPNPRT'

'END'

```

6661 *Betatron damping*

6662 Figure 20.62 shows the damped vertical motion of the individual particles, over
 6663 the acceleration range, together with the initial and final distributions of the 11
 6664 particles on elliptical invariants. Departure from the matching ellipse at the end of
 6665 the acceleration cycle, 3 GeV (Eq. 20.14 with $\epsilon_Z/\pi = 1.0745 \times 10^{-6}$ m), is marginal.

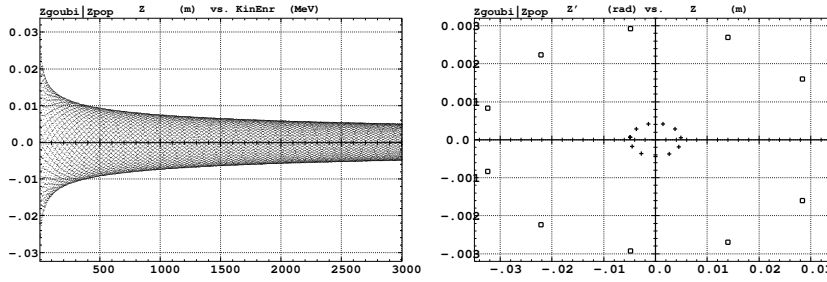


Fig. 20.62 Left: damped vertical motion, from 3.6 MeV to 3.004 GeV in 30,000 turns. Right: the initial coordinates of the 11 particles (squares) are taken on a common invariant $\epsilon_Z(0) = 10^{-4} \pi$ m (at 3.6 MeV, $\beta\gamma = 0.0877$, thus $\beta\gamma\epsilon_Z(0) = 8.77 \times 10^{-6} \pi$ m); the final coordinates after 30,000 turns (crosses) appear to still be (with negligible departure) on a common invariant of value $\epsilon_Z(\text{final}) = 2.149 \times 10^{-6} \pi$ m (at 3.004 GeV, $\beta\gamma = 4.08045$) thus $\beta\gamma\epsilon_Z(\text{final}) = 8.77 \times 10^{-6} \pi$ m, equal to the initial value

6666 *Degree of non-symplecticity of the numerical integration*

6667 The degree of non-symplecticity as a function of integration step size is illustrated
 6668 in Fig. 20.63. The initial motion is taken paraxial, vertical motion is considered as
 6669 it resorts to off-mid plane Taylor expansion of fields [1, DIPOLE Sec.], a stringent
 6670 test as the latter is expected to deteriorate further the non-symplecticity inherent
 6671 to the Lorentz equation integration method (a truncated Taylor series method [1,
 6672 Eq. 1.2.4]).

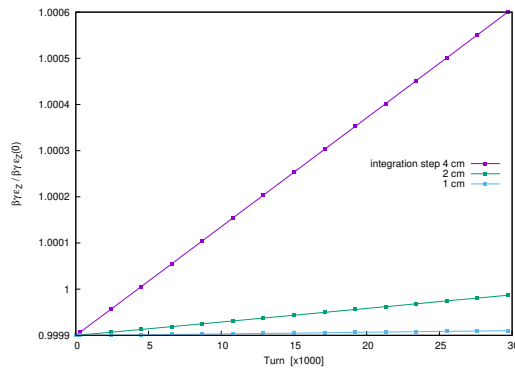
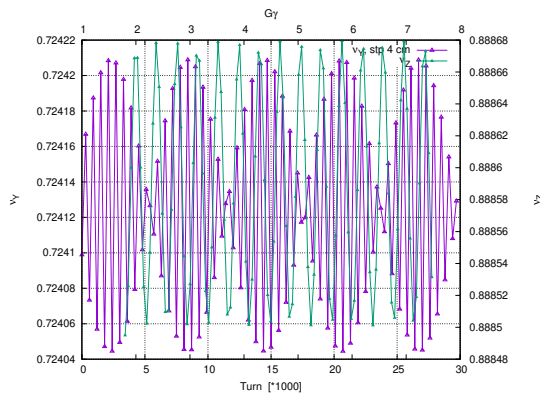


Fig. 20.63 Turn-by-turn evolution of the normalized invariant, $\beta\gamma e_z(\text{turn})/\beta\gamma e_z(0)$ (initial $e_z(0)$ taken paraxial), for four different integration step size values: 1, 2 and 4 cm

6673 *Evolution of the wave numbers*

6674 The Fortran tool `tunesFromFai_iterate` can be used to compute tunes as a function
 6675 of turn number or energy, it reads turn by turn particle data from `zgoubi.fai` and
 6676 computes a discrete Fourier transform over so many turns (a few tens, 100 here
 6677 for instance), every so many turns (300, here) [4]. Typical results are displayed in
 6678 Fig. 20.64, tunes have the expected values: $\nu_Y = 0.7241$, $\nu_Z = 0.8885$. In acceleration
 6679 rate of 100 keV/turn has been taken (namely, $\hat{V} = 200$ kV and still $\phi_s = 150^\circ$), to
 6680 save on computing time. SCALING with option `NTIM=-1` causes the magnet field
 6681 to strictly follow the momentum boost by `CAVITE`.

Fig. 20.64 Horizontal ring tune (left vertical axis), $\nu_Y \approx 0.7241$, and vertical ring tune (right vertical axis), $\nu_Z \approx 0.8885$, as a function of turn number, over 30,000 turns ($E : 0.0036 \rightarrow 3$ GeV at a rate of 100 keV/turn)



6682 (f) Spin tracking. Bunch polarization.

Spin depolarizing resonances in Saturne I synchrotron are located at (Figs. 20.65, 20.66)

$$G\gamma_R = k \pm \nu_Z = k \pm 0.888284 \quad \equiv 4 - 0.888284, 4 + 0.888284, 8 - 0.888284$$

6683 where ν_Z has been taken from Tab. 20.50, or from Fig. 20.64. $G\gamma_R$ is bounded by
6684 $G\gamma(3 \text{ GeV}) = 7.525238 < 8 + \nu_Z$

6685 The simulation data file to track through these resonances is the same as in
6686 question (e), Tab. 20.54, except for the following substitutions:

- 6687 - substitute MCOBJET (to be uncommented) to OBJET (to be commented),
- 6688 - under CAVITE substitute a peak voltage $V = 20 \text{ kV}$ to $V = 200 \text{ kV}$,
- 6689 - under REBELOTE, request a 300,000 turn cycle rather than 30,000.

MCOBJET creates a 200 particle bunch with Gaussian transverse and longitudinal densities, with the following *rms* values at 3.6 MeV:

$$\epsilon_Y/\pi = 25 \mu\text{m}, \quad \epsilon_Z/\pi = 10 \mu\text{m}, \quad \frac{dp}{p} = 10^{-4}$$

6690 CAVITE accelerates that bunch from 3.6 MeV to 3 GeV at a rate of $q\hat{V} \sin(\phi_s) =$
6691 10 keV/turn ($\hat{V} = 20 \text{ kV}$, $\phi_s = 30^\circ$), in 300,000 turns.

6692 Figure 20.65 shows sample S_Z spin components of a few particles taken among
6693 the 200 tracked. Figure 20.66 displays $\langle S_Z \rangle$, the vertical polarization component of
6694 the 200 particle set. A gnuplot script is used, given in Tab. 20.55.

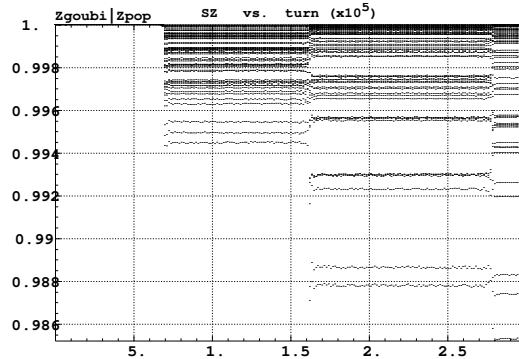


Fig. 20.65 Vertical spin component of a few particles accelerated from 3.6 MeV to 3 GeV. This plot is obtained using zpop, which reads data from [b_]zgoubi.fai: menu 7; 1/2 to open b_zgoubi.fai; 2/[20,23] to select S_Z versus turn; 7 to plot

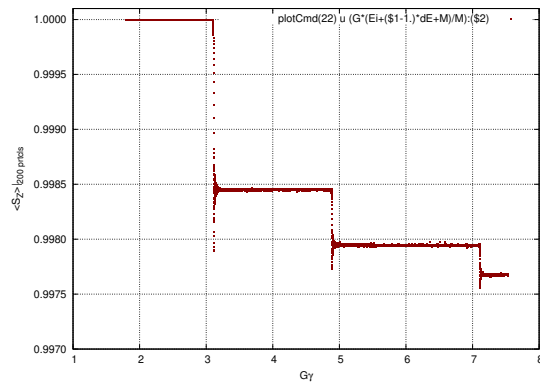


Fig. 20.66 Average vertical spin component of a 200 particle bunch, accelerated from 3.6 MeV to 3 GeV

Table 20.55 A gnuplot script to plot the average vertical spin component of the 200 particle set, along the acceleration ramp (Fig. 20.66). The average is prior computed by an awk script, which reads the necessary data from zgoubi.fai.

```
# gnuplot_avrgFromFai.gnu
 fName = 'zgoubi.fai'; plotCmd(col_num)=sprintf('< gawk -f average.awk -v col_num=%d %s', col_num, fName)
 set xtics; set ytics; set xlabel "G{/Symbol g}"; set ylabel "<S_z>|_{200 prtcls}"
 set format y "%0.4f"; set grid; set xr [:]; set yr [0.997:1.0001]
 Qy=0.888248;
 do for [intgr=1:2] { set arrow nohead from 4*intgr-Qy, 0.997 to 4*intgr+Qy, 1.0001 lw 1 dt 2
                      set arrow nohead from 4*intgr+Qy, 0.997 to 4*intgr+Qy, 1.0001 lw 1 dt 2 }
 M=938.27208; Ei = 3.6; G = 1.79284735; Qy = 0.888248; dE = 0.01 # MeV/turn
 plot plotCmd(22) u (G*(Ei+($1-1)*dE+M)/M):($2) w p pt 5 ps .4 lc rgb 'dark-red'; pause 1
```

average.awk script to compute $\langle S_z \rangle$ [5]:

```
function average(x, data){
  n = 0; mean = 0;
  val_min = 0; val_max = 0;
  for(val in data){
    n += 1;
    delta = val - mean;
    mean += delta/n;
    val_min = (n == 1)?val:((val < val_min)?val:val_min);
    val_max = (n == 1)?val:((val > val_max)?val:val_max);
  }
  if(n > 0){
    print x, mean, val_min, val_max;
  }
}
{
  curr = $38;
  yval = $(col_num);

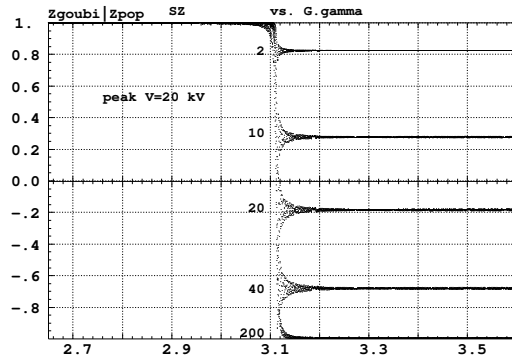
  if(NR==1 || prev != curr){
    average(prev, data);
    delete data;
    prev = curr; }
  data[yval] = 1; }
END{
  average(curr, data); }
```

- 6695 (g) Crossing an isolated intrinsic depolarizing resonance.
 6696 The simulation uses the file given in Tab. 20.54, with the following changes:
- 6697 • Under OBJET:
 - 6698 – 1st line, change the reference rigidity to $BORO = 4.08807740024$ T m
 - 6699 which corresponds to an initial $G\gamma = 2.65$, 448.604769 MeV (in lieu of
 - 6700 0.274426548 T m, 3.6 MeV), which is conveniently upstream of $G\gamma_R =$
 - 6701 $4 - \nu_Z \approx 3.1$,
 - 6702 – 3rd line, request a single particle (“1 1 1”, in lieu of “1 11 1” which distributes
 - 6703 11 particles on the vertical invariant),
 - 6704 – 6th line, set the invariant ϵ_Z/π to the desired value,
 - 6705 • change the dipole field accordingly under DIPOLE, to 4.85560248505 T (in
 - 6706 lieu of 0.3259493638 T), which maintains the expected curvature radius $\rho_0 =$
 - 6707 $BORO/B = 8.4193$ m (Tab. 9.2),
 - 6708 • under REBELOTE, set the number of turns. A total of 15,000, about 7,500 turns
 - 6709 upstream and as many downstream of the resonance, is convenient for the present
 - 6710 peak voltage $\hat{V} = 20$ kV (acceleration rate 20 keV/turn).

6711 *Changing the particle invariant value*

- 6712 Particle spin motion through the isolated resonance for five different invariant values,
 6713 $\epsilon_Z/\pi = 2, 10, 20, 40, 200 \mu\text{m}$, is displayed in Fig.20.67.

Fig. 20.67 Turn by turn spin motion through the isolated resonance $G\gamma_R = 4 - \nu_Z$, observed at the beginning of the optical sequence (FAISTORE location, Tab. 20.54) for six different values of the particle invariant from $2 \mu\text{m}$ to $200 \mu\text{m}$ where full spin flip occurs. A graph obtained using zpop, which reads particle data from b_polarLand.fai (as specified under FAISTORE): menu 7; 1/8 to choose b_polarLand.fai; 2/[59,23] to select S_Z versus $G\gamma$; 7 to plot



- 6714 The intrinsic resonance strength satisfies $\epsilon_R^2 = A \epsilon_Z$, with A a factor which char-
 6715 acterizes the lattice. On the other hand, from the Froissart-Stora formula (Eq. 9.45)
 6716 one gets

$$\epsilon_R^2 = \frac{2\alpha}{\pi} \ln \left(\frac{2}{1 + S_{Z,f}/S_{Z,i}} \right) \xrightarrow{\frac{S_{Z,f}}{S_{Z,i}} \ll 1} \frac{\alpha}{\pi} \left(1 - \frac{S_{Z,f}}{S_{Z,i}} \right) \quad (20.15)$$

6717 with α , crossing speed, a constant. Thus one expects to find $\ln\left(\frac{2}{1+S_{Z,f}/S_{Z,i}}\right) / \epsilon_Z$
 6718 constant. This property appears to be satisfied by the tracking outcomes, Tab. 20.56.
 6719 Note that numerical results slowly depart from that rule if $P_f/P_l \rightarrow 1$ or when
 6720 approaching full flip, explaining this variation requires closer inspection of the
 6721 theory and dedicated simulations.

6722 Calculation of the resonance strength from the P_f/P_l tracking results, using
 6723 Eq. 20.15, requires the crossing speed, namely,

$$\alpha = \frac{1}{2\pi} \frac{\Delta E}{M} = \frac{1}{2\pi} \frac{20 \times 10^3 \times \sin 30^\circ \text{ [eV/turn]}}{938.27208 \times 10^6 \text{ [eV]}} = 1.696 \times 10^{-6} \quad (20.16)$$

6724 Table 20.56, rightmost column, displays the ratio $|\epsilon_R|/\sqrt{\epsilon_Z/\pi}$ so obtained. The
 6725 resonance strength $|\epsilon_R|$ appears to be proportional to $\sqrt{\epsilon_Z/\pi}$, this is the expected
 result [6].

Table 20.56 Relationship between the invariant value ϵ_Z/π and the quantity $\ln\left(\frac{2}{1+S_{Z,f}/S_{Z,i}}\right) \propto |\epsilon_R|$. $\hat{V} = 20$ kV, here. $S_{Z,f}/S_{Z,i}$ (col. 2) is from raytracing, ϵ_R^2 results, using Eq. 20.15 with crossing speed $\alpha = 1.696 \times 10^{-6}$ (Eq. 20.16). The resulting ratio $\epsilon_R^2 / \epsilon_Z/\pi$, rightmost column, appears to be about constant, this is the expected result (Eq. 20.15)

ϵ_Z/π ($\times 10^{-4} \mu\text{m}$)	$\frac{S_{Z,f}}{S_{Z,i}} \equiv S_{Z,f}$	$\ln \frac{2}{1+S_{Z,f}}$	$\frac{\ln \frac{2}{1+S_{Z,f}}}{\epsilon_Z/\pi}$	$\frac{\epsilon_R^2}{\epsilon_Z/\pi}$ ($\times 10^{-8}$)
1	+0.9	0.0513	0.0513	5.5
2	+0.822	0.0932	0.0466	5.0
10	+0.27	0.454	0.0454	4.9
20	-0.19	0.904	0.0452	4.9
40	-0.68	1.833	0.0458	4.9
50	-0.775	2.19	0.438	4.7
80	-0.963	3.297	0.0412	4.5

6726

6727 *Changing the crossing speed*

6728 A crossing case using $\hat{V} = 10$ kV is displayed in Fig. 20.68. an acceleration
 6729 rate/resonance crossing speed twice as slow compared to the previous ones.

6730 Comparison with the case $\hat{V} = 20$ kV is given in Tab. 20.57. From what
 6731 precedes, with the crossing speed $\alpha \propto \hat{V} \propto \Delta E/\text{turn}$, one expects to find
 6732 $\frac{\hat{V}}{\epsilon_Z/\pi} \times \ln\left(\frac{2}{1+S_{Z,f}/S_{Z,i}}\right) = \text{constant}$. This property appears to be satisfied by track-
 6733 ing outcomes, Tab. 20.57.

Fig. 20.68 Turn by turn spin motion through the isolated resonance $G\gamma_R = 4 - \nu_Z$, observed at the beginning of the optical sequence (FAIS-TORE location, Tab. 20.54) for $\epsilon_Z/\pi = 1 \mu\text{m}$ and $20 \mu\text{m}$. $\hat{V} = 20 \text{ kV}$. A graph obtained using zpop, which reads particle data from b_polarLand.fai (as specified under FAIS-TORE): menu 7; 1/8 to choose b_polarLand.fai; 2/[59,23] to select S_Z versus $G\gamma$; 7 to plot

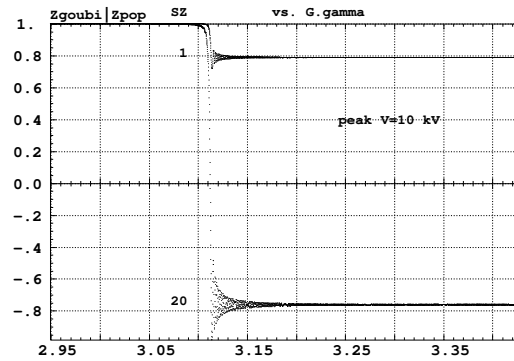


Table 20.57 Relationship between the acceleration rate $\Delta E \propto \hat{V}$ and the quantity $\ln \left(\frac{2}{1+S_{Z,f}/S_{Z,i}} \right)$. Normalized to ϵ_Z/π , their product (rightmost column) appears about constant, this is the expected result. Explaining the observed $\approx 10\%$ variation requires closer inspection of the theory and dedicated simulations

ϵ_Z/π ($\times 10^{-4} \mu\text{m}$)	\hat{V} (kV)	$\frac{S_{Z,f}}{S_{Z,i}} \equiv S_{Z,f}$	$\ln \frac{2}{1+S_{Z,f}}$	$\frac{\hat{V}}{\epsilon_Z/\pi} \times \ln \frac{2}{1+S_{Z,f}}$
1	10	+0.79	0.111	1.1
20	10	-0.763	2.133	1.07
1	20	+9	0.051	1.0
2	20	+0.82	0.094	0.94

6734 (h) Spin motion across a weak depolarizing resonance.

6735 The goal is to check numerical outcomes against the Fresnel integral model
6736 (Eq. 9.51). A weak resonance is obtained using small amplitude vertical motion and
6737 fast crossing.

6738 A single particle is raytraced, in the following conditions:

- 6739 - resonance to be crossed: $G\gamma_R = 4 - \nu_y \approx 3.1115$,
- 6740 - acceleration: peak voltage $\hat{V} = 100$ kV, synchronous phase $\phi_s = 30^\circ$,
- 6741 - particle invariant $\epsilon_Z/\pi = 10^{-6}$ μm .

6742 The initial rigidity is taken a few hundred turns upstream of the resonance, namely,
6743 $B\rho_{\text{ref}} = 4.0880774$ T m, 605226550 MeV, $G\gamma = 2.94931241$, a distance to $G\gamma_R$ of
6744 $4 - \nu_Z - 2.94931241 \approx 0.16223$. Tracking extends a few thousand turns beyond
6745 $G\gamma_R$ so that S_Z reaches its asymptotic value, from which the resonance strength $|\epsilon_R|$
6746 can be calculated, using Eq. 20.15.

6747 The simulation file is given in Tab. 20.58. Note the new setting of the SCALING
6748 factor SCL: DIPOLE field was set for a curvature radius $\rho_0 = 8.4193$ m, given a
6749 reference rigidity $B\rho_{\text{ref}} \equiv \text{BORO} = 0.274426548$ Tm (Tab. 20.46). However the
6750 reference rigidity is now changed to $B\rho_{\text{ref}} = 4.0880774$ T m, thus maintaining ρ_0
6751 requires scaling the field in DIPOLE by $4.0880774/0.274426548 = 14.8968$ at turn
6752 1: this is the new factor, $SCL = 14.8968$, under SCALING (Tab. 20.58). Option
6753 NT=-1 under SCALING ensures that the scaling factor will automatically follow,
6754 turn-by-turn, the rigidity boost by CAVITE so preserving constant curvature radius
6755 $\rho_0 = 8.4193$ m.

6756 The resulting turn-by-turn spin motion is displayed in Fig. 20.69. The Fresnel
6757 integral model (Eq. 9.51) has been superimposed. Parameters in the latter are as
6758 follows:

- 6759 - crossing speed $\alpha = \frac{1}{2\pi} \frac{\Delta E}{M} = \frac{1}{2\pi} \frac{10^5 \times \sin 30^\circ [\text{eV/turn}]}{938.27208 \times 10^6 [\text{eV}]} = 8.4812 \times 10^{-6}$,
- asymptotic $S_{Z,f} = 0.999780$, whereas initial $S_{Z,i} = 1$, thus (Eq. 20.15)

$$\epsilon_R^2 = 5.939 \times 10^{-10}$$

- 6760 - orbital angle origin set at the location of $G\gamma_R$, which is turn 1699.

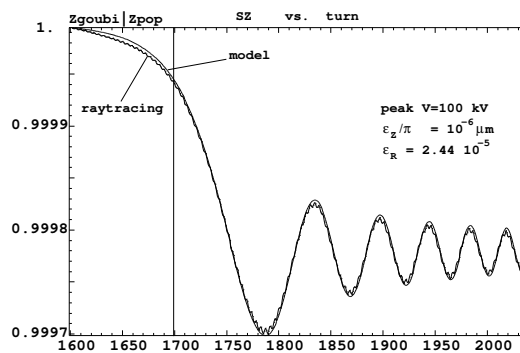


Fig. 20.69 Turn by turn spin motion through the isolated resonance $G\gamma_R = 4 - \nu_Z$, case of weak resonance strength. Modulated curve: from raytracing. Smooth curve: from the Fresnel integral model

Table 20.58 Simulation input data file: track a particle launched on a vertical invariant $\epsilon_y/\pi = 10^{-6} \mu\text{m}$, with horizontal motion indifferent, taken zero here. The INCLUDE adds the Saturne I cell four times, the latter is defined in Tab. 20.48 and Fig. 9.23

```

Saturne I ring. Crossing Ggamma=4-nu_Z, weak resonance case (small vertical invariant)
'MARKER' SatIWeakXing_S ! Just for edition purposes.
'OBJET'
4.08807740024e3 ! Reference Brho: 605226550 MeV proton.
8 ! Create a (set of) particle(s) on a given invariant.
1 1 1 ! create a single particle.
0. 0. 0. 0. 0. 1.
0. 14.426 0 ! Horizontal invariant is null.
0. 11.411 1e-6 ! Periodic alpha_Z, beta_Z, and invariant value.
0. 1. 0. ! No momentum spread.
'PARTICUL'
PROTON ! Necessary data in order to allow (i) spin trackingand, and (ii) acceleration.
'SPNTRK' ! Switch on spin tracking,
3 ! nitial spin vertical.
'FAISCEAU'
'FAISTORE'
xing4-Qy.fai ! Log particle data in xing.fai, turn-by-turn.
1

'SCALING'
1 1
DIPOLE
-1 ! Causes field increase in DIPOLE to follow rigidity increase by CAVITE.
14.8968 ! Relative rigidities at turn 1.
1

! 4 cells follow.
'INCLUDE'
1
4* ./SatI_cell.inc[S_SatI_cell:E_SatI_cell]

'CAVITE'
3
0 0
100e3 0.523598775598 ! Acceleration rate is 200*0.5=100keV/turn.

'REBELOTE'
3999 0.3 99 ! A total of 3999+1=4000 turns.

'FAISCEAU'
'MARKER' SatIWeakXing_E ! Just for edition purposes.
'SPNPRT'

'END'

```

6761 (i) Static spin motion near a resonance

6762 The simulation input data file of Tab. 20.58 can be used for these fixed energy
6763 trials, however OBJET[KOBJ=8] has to be changed, as follows:

6764 - OBJET[KOBJ=1] is used instead, as it allows to define a set of particles with
6765 sampled momentum offset,

6766 - the reference rigidity in OBJET is set closest to the resonance, $G\gamma_R = 4 -$
6767 $\nu_y \approx 3.1115$ (considering that $\nu_Z \approx 0.8885$ (Fig. 20.64), thus $BORO \equiv B\rho_{\text{ref}} =$
6768 4.439362178 . Note that $G\gamma_R = 4 - \nu_Z$ is only known at the accuracy that ν_Z is, from
6769 prior first order mapping computation, or Fourier analysis; finding the resonant $G\gamma_R$
6770 from spin motion will bring its value

6771 - the SCALING factor is set to $SCL = 1$ and concurrently the DIPOLE field is
6772 set to $B_0 = 5.27283999437$,

6773 - since half an oscillation of $S_Z(\text{turn})$ is enough to determine $\langle S_Z \rangle$, a number of
6774 turns $IPASS \approx$ a few thousand, under REBELOTE, is enough considering the verti-
6775 cal motion amplitude considered. considering the initial $Z=3$ cm in this simulations
6776 (thus $\epsilon_Z/\pi = Z^2/\beta_Z = 79 \cdot 10^{-6}$ with $\beta_Z = 11.411$ (Tab. 20.49)), $IPASS = 3000$ is
6777 enough.

6778 To conclude on this updating of the input data file of Tab. 20.58:

6779 - substitute the following to OBJET:

```
6780 'OBJET'
6781 4.4393621786553803e3 ! BORO taken as close to resonant G.gamma as prior knowledge of nu.Z allows.
6782 1 ! Create a set of particles.
6783 1 1 1 1 1 41 ! 41 particles sampling a
6784 0. 0. 0. 0. 0. .00001 ! momentum offset, in -20*1e-5< D-1 < 20*1e-5.
6785 0. 0. 3. 0. 0. 1. ! All particles have initial Z=3cm.
6786
```

6787 - substitute the following to SCALING:

```
6788 'SCALING'
6789 1 1
6790 DIPOLE
6791 -1 ! Causes field increase in DIPOLE, in correlation to particle
6792 1. ! rigidity increase by CAVITE.
6793 1
6794
```

6795 - substitute the following for B_0 (3rd line) under DIPOLE:

```
6796 22.5 5.27283999437 -0.6 0. 0. ! Reference angle ACENT set to AT/2; Bo field at RM; radial index.
6797
```

6798 The turn-by-turn values of the vertical component of the spins as they pre-
6799 cess at fixed energy are displayed in Fig. 20.70. A quick, and accurate enough,
6800 approximation to the vertical component of the precession axis is $\langle S_Z \rangle|_{\text{period}} =$
6801 $\frac{1}{2} \{ \min [S_Z(\theta)] + \max [S_Z(\theta)] \}$, it yields the $\langle S_Z \rangle (\Delta)$ graph of Fig. 20.71.

A match of the $\langle S_Z \rangle$ values by (Eq. 9.49)

$$S_y(\Delta) = \frac{\Delta}{\sqrt{\Delta^2 + |\epsilon_R|^2}}$$

given $G\gamma_R = 4 - \nu_Z$, yield vertical tune and resonance strength values, respectively,

$$\nu_Z = 0.88845 \quad \text{and} \quad |\epsilon_R| = 2.77 \times 10^{-4}$$

6802 Satisfactorily, ν_Z is consistent with earlier results, and $|\epsilon_R| = 2.77 \times 10^{-4}$ for $\epsilon_Z/\pi =$
6803 79×10^{-6} here, is consistent in order of magnitude with $|\epsilon_R| = 2.44 \times 10^{-5}$ for

Fig. 20.70 Turn-by-turn value of the vertical component of spins precessing at fixed energy in Saturne I synchrotron, observed at the beginning of the sequence, where spins start vertical ($S_Z = 1$). The greater (respectively smaller) the distance to the resonance, the closer the precession axis to the vertical axis (resp., to the bend plane), and the greater (resp. the smaller) the oscillation frequency

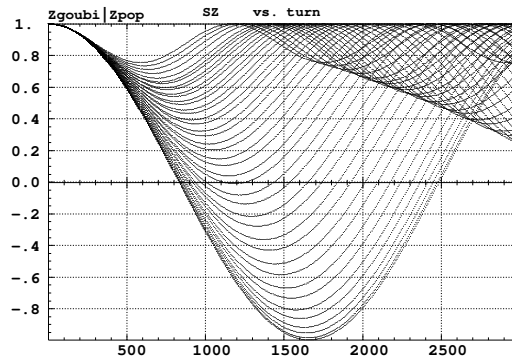
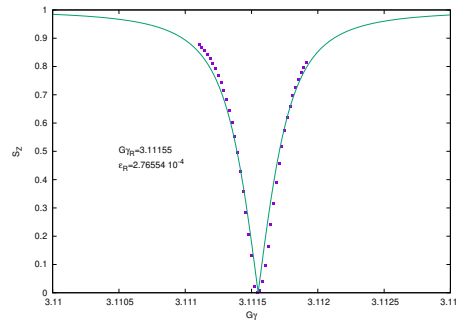


Fig. 20.71 Vertical component of the spin precession axis as a function of $G\gamma$, in the vicinity of the resonance



6804 $\epsilon_Z/\pi = 10^{-6}$ in the previous question (h). The difference deserves further inspection,
 6805 a possible additional question in this exercise.

6806 **9.2**6807 **Construct the ZGS. Spin Resonances**

6808 A photo taken in the ZGS ring can be found in Fig. 9.4. A schematic layout is
 6809 given in Fig. 9.24 and a sketch of the double dipole cell in Fig. 9.25. These figures
 6810 introduce to the geometry and, in complement to Tab. 9.3, display some of the
 6811 parameters of the synchrotron, and will be referred to in building the ZGS ring in the
 6812 following.

6813 (a) A model of ZGS synchrotron.

6814 DIPOLE is used to simulate the cell dipoles. It is necessary to have Fig. 20.55 at
 6815 hand (in addition to the users' guide), when filling up the data list under DIPOLE.
 6816 Some comments regarding these data:

- 6817 • DIPOLE is defined in a cylindrical coordinate system.
- 6818 • The bending sector is 45 degrees, however the field region extent AT has to
 6819 encompass the fringe fields, at both ends of the 45 deg sector. A large 5 deg
 6820 extension is taken, for a total AT=55 deg which ensures absence of truncation of
 6821 the fringe fields at the AT sector boundaries, over the all radial excursion of the
 6822 beam.
- 6823 • RM is given the curvature radius value, $RM = B\rho/B = 1.035270_{[T.m]}/0.04986851_{[T]} =$
 6824 20.76 m, this makes magnet positioning and closed orbit checks easier (see be-
 6825 low). Note that the field and reference rigidity are, as for the simulation input
 6826 data, for 50 MeV, the injection energy, this is an arbitrary choice.
- 6827 • ACENT=27.5 deg is the reference azimuth, for the positioning of the entrance and
 6828 exit effective field boundaries (EFB). It is taken in the middle of the AT range, an
 6829 arbitrary choice.
- 6830 • The entrance radius in the AT sector is $RE = RM/\cos(AT - \omega^+) = RM/\cos(5^\circ)$,
 6831 with $\omega^+ = 22.5$ deg the positioning of the entrance EFB with respect to ACENT.
 6832 And similarly for the positioning of the exit reference frame, $RS = RM/\cos(AT -$
 6833 $(ACENT - \omega^-)) = RM/\cos(5^\circ)$ with $\omega^- = -22.5$ deg the positioning of the exit
 6834 EFB. Note that $\omega^+ - \omega^- = 45^\circ$, the value of the bend angle.
- 6835 • The entrance angle TE identifies with the extension to the 45 deg sector, namely,
 6836 TE=5 deg. And similarly for the positioning of exit frame, 5 deg downstream of
 6837 the exit EFB, thus TS=5 deg.

6838 In order to build the cell, and in the first place the two cell dipole (the two dipoles
 6839 are mirror symmetric, thus build one, the other follows straightforwardly), it is a
 6840 good idea to proceed by steps:

6841 (i) first build a 45 deg deviation sector in the hard edge model (Tab. 20.59).
 6842 FAISCEAU located next to DIPOLE indicates that a trajectory entering DIPOLE
 6843 at radius R=RM, normally to the EFB (thus, $Y_0 = 0$ and $T_0 = 0$ in OBJET) exits
 6844 with Y=0 and T=0. Data validation at this stage can be performed by comparing
 6845 DIPOLE's transport matrix computed with MATRIX, and the theoretical expectation
 6846 (after Eq. ??, Sec. 19.5, numerical values truncated to 4th decimal)

$$T = \begin{pmatrix} \cos \alpha & \rho \sin \alpha & 0 & 0 & 0 & \rho(1 - \cos \alpha) \\ -\frac{1}{\rho} \sin \alpha & \cos \alpha & 0 & 0 & 0 & \sin \alpha \\ 0 & 0 & 1 & \rho \alpha & 0 & 0 \\ 0 & 0 & 0 & 1 & 0 & 0 \\ \sin \alpha & 0 & 0 & 0 & 1 & \rho(\alpha - \sin \alpha) \\ 0 & 0 & 0 & 0 & 0 & 1 \end{pmatrix} \xrightarrow[\rho=20.76]{\alpha=\pi/4} \begin{pmatrix} 0.7071 & 14.6795 & 0 & 0 & 0 & 6.0804 \\ -0.03406 & 0.7071 & 0 & 0 & 0 & 0.7071 \\ 0 & 0 & 1 & 16.3048 & 0 & 0 \\ 0 & 0 & 0 & 1 & 0 & 0 \\ 0.7071 & 0 & 0 & 0 & 1 & 1.6253 \\ 0 & 0 & 0 & 0 & 0 & 1 \end{pmatrix}$$

6847 MATRIX computation outcomes from raytracing can be found for comparison in Tab. 20.60.

Table 20.59 Simulation input data file: a 45 degree sector bend in the hard edge model. The reference trajectory has equal entrance and exit position, and opposite sign angles. It coincides with the arc $R=RM$. MATRIX computes the transport matrix of the dipole (bottom of this Table), for comparison with the fringe field model, and possible comparison with matrix codes outcomes

```

ZGS. Hard edge dipole model. Transport matrix.
'OBJET'
1.03527036749193e3                               ! Reference Brho: 50 MeV proton.
5                                                    ! Create an 11 particle set, proper for MATRIX computation.
.001 .01 .001 .01 .001 .0001                       ! Coordinate sampling.
0. 0. 0. 0. 0. 1. 'o'                             ! Reference trajectory: all initial coordinates nul, relative rigidity D=1.
1
'DIPOLE'                                           ! Analytical modeling of a dipole magnet.
20                                                  ! IL=2 here, to log trajectory coordinates in zgoubi.plt, at integration steps.
45. 2076.                                           ! Field region angle=45; reference radius set to curvature radius value.
22.5 0.4986851481175 0. 0. 0. ! Reference angle ACENT set to AT/2; Bo field at RM; indices, all zero.
.0 0.                                               ! EFB 1 with fringe field extent.
4 .1455 2.2670 -.6395 1.1558 0. 0. 0.           ! Enge coefficients.
22.5 0. 1.E6 -1.E6 1.E6 1.E6                     ! Angle to ACENT; face angle; face is straight.
0 0.                                               ! EFB 2.
4 .1455 2.2670 -.6395 1.1558 0. 0. 0.           ! Enge coefficients.
-22.5 0. 1.E6 -1.E6 1.E6 1.E6                    ! Angle to ACENT; face angle; face is straight.
0 0.                                               ! EFB 3. Unused.
0 0. 0. 0. 0. 0. 0. 0. 0. 0. 0. 0.             ! EFB 3. Unused.
0 0. 1.E6 -1.E6 1.E6 1.E6 0.
2 1                                                ! Degree of interpolation polynomial; flying grid sizing.
200.                                               ! Integration step size. It can be large in uniform field.
2 2076. 0. 2076. 0.                               ! Positioning of entrance and exit frames.
! reference frames.
'FAISCEAU'                                         ! Local particle coordinates.
'MATRIX'                                           ! Compute transport matrix, from trajectory coordinates.
1 0
'END'

```

6848

6849 (ii) next, add fringe fields, including the 5 deg extensions that add to AT
6850 (Tab. 20.61). Note that negative drifts with length $RM \tan(5^\circ) = 181.62646548$ cm
6851 have been added at both ends, this recovers the actual length of the trajec-
6852 tory across the 45 deg sector, for comparison with the hard-edge case, namely,
6853 $s = 16.30486 \pm 10^{-5}$ m under FAISCEAU in both cases. A FIT procedure finds
6854 the field value necessary for recovering the exact deviation, as the latter is changed
6855 when fringe fields are introduced. Again, FAISCEAU allows checking the correct-
6856 ness of DIPOLE data: exit coordinates come out to be $Y=0$ and $T=0$; however the
6857 path across the dipole is changed under the effect of the fringe fields, thus its length
6858 ($s=1630.459$ cm) is slightly different, compared to the hard edge case (an arc of
6859 radius radius $RM=2076$ cm and length 1630.487 cm)

(iii) next, add the EFB angles: the sector is closing (wedge angles $\epsilon_1 > 0$ and $\epsilon_2 > 0$ by convention) thus the EFB tilt angle θ under DIPOLE if positive at entrance, negative at exit (Fig. 20.55). In order to reach proper wave number values (this is addressed below), the wedge angles are taken to be $\epsilon_1 = 13^\circ$ and $\epsilon_2 = 8^\circ$. These considerations result in the following:

Table 20.60 Outcomes of the simulation file of Tab. 20.59

An excerpt from *zgoubi.res*. Coordinates of the first particle (the reference trajectory) and its path length under FAISCEAU, at OBJET on the left hand side below, locally on the right hand side:

```

3 Keyword, label(s) : FAISCEAU                                     IPASS= 1
                                     TRACE DU FAISCEAU
                                     (follows element # 2)
                                     11 TRAJECTOIRES
OBJET
D      Y(cm)  T(mr)  Z(cm)  P(mr)  S(cm)  D-1  Y(cm)  T(mr)  Z(cm)  P(mr)  S(cm)
0 1  1.0000  0.000  0.000  0.000  0.000  0.0000  0.0000  -0.000  -0.000  0.000  0.000  1.630487E+03

```

Transport matrix of a 45 degree sector, hard edge model, two difference cases of integration step size, namely, 4 cm and 2 m (an excerpt of MATRIX computation, from *zgoubi.res*). It can be checked against matrix transport expectations. The “first order symplectic conditions” are very small in the 4 cm step size case, which is an indication of accurate numerical integration of the trajectories across DIPOLE; the reference trajectory (first one) exits better aligned (reference coordinates, before change of frame for MATRIX computation, are closer to zero):

- Case of 4 cm step size:

```

4 Keyword, label(s) : MATRIX                                     IPASS= 1
Reference, before change of frame (particle # 1 - D-1,Y,T,Z,s,time) :
0.00000000E+00 -3.25144356E-10 -4.13789229E-10 0.00000000E+00 0.00000000E+00 1.63048659E+03 5.43871783E-02

TRANSFER MATRIX ORDRE 1 (MKSA units)
0.707107 14.6795 0.000000 0.000000 0.000000 0.000000 6.08046
-3.406102E-02 0.707107 0.000000 0.000000 0.000000 0.000000 0.707107
0.000000 0.000000 1.000000 16.3049 0.000000 0.000000 0.000000
0.000000 0.000000 7.285552E-16 1.000000 0.000000 0.000000 0.000000
0.707107 6.08046 0.000000 0.000000 0.000000 1.000000 1.62533
0.000000 0.000000 0.000000 0.000000 0.000000 0.000000 1.000000

DetY-1 = 0.0000000025, DetZ-1 = 0.0000000002
T12=0 at -20.76 m, T34=0 at -16.30 m
First order symplectic conditions (expected values = 0) :
2.5100E-09 2.3381E-10 0.000 0.000 0.000 0.000

```

- Case of 2 m step size:

```

4 Keyword, label(s) : MATRIX                                     IPASS= 1
Reference, before change of frame (particle # 1 - D-1,Y,T,Z,s,time) :
0.00000000E+00 -2.01277929E-03 -2.51514609E-03 0.00000000E+00 0.00000000E+00 1.63048722E+03 5.43871994E-02

TRANSFER MATRIX ORDRE 1 (MKSA units)
0.707105 14.6795 0.000000 0.000000 0.000000 0.000000 6.08056
-3.406102E-02 0.707108 0.000000 0.000000 0.000000 0.000000 0.707120
0.000000 0.000000 1.000000 16.3051 0.000000 0.000000 0.000000
0.000000 0.000000 1.457135E-17 1.00003 0.000000 0.000000 0.000000
0.707109 6.08048 0.000000 0.000000 0.000000 1.000000 1.62531
0.000000 0.000000 0.000000 0.000000 0.000000 0.000000 1.000000

DetY-1 = -0.000010903, DetZ-1 = 0.0000286273
R12=0 at -20.76 m, R34=0 at -16.30 m
First order symplectic conditions (expected values = 0) :
-1.0903E-06 2.8627E-05 0.000 0.000 0.000 0.000

```

- the entrance (respectively exit) EFB of the upstream dipole of the cell (Fig. 9.25) is tilted with respect to the reference orbit by an angle $\theta = +13^\circ$ (resp. $\theta = -8^\circ$),

- the entrance (resp. exit) EFB of the downstream dipole is tilted with respect to the reference orbit by an angle $\theta = +8$ deg (resp. $\theta = -13^\circ$).

This final step requires again re-adjusting the radial positioning of the dipole (RE and RS, entrance and exit radius respectively), and field. In that aim the FIT procedure in Tab. 20.61 is added a variable: the RE and RS radii, coupled, and a constraint: the reference orbit has zero radial excursion at exit of the dipole. This FIT results in

Table 20.61 Simulation input data file: ZGS 45deg sector bend, with entrance and exit EFBs wedge angles and fringe fields. The reference trajectory has equal entrance and exit position, and opposite sign angles. It runs closely to the arc $R=RM$, not strictly coinciding with the latter due to the fringe fields. MATRIX computes the transport matrix of the dipole, for comparison with the hard edge model. Negative drifts with length $RM \tan(5^\circ) = 181.62646548$ cm are added to recover the hard edge path length

```
ZGS. Simplified model. Find centered orbit in DIPOLE.
'OBJET'
1.03527036749193e3                               ! Reference Brho: 50 MeV proton.
5                                                    ! Create an 11 particle set, proper for MATRIX computation.
.001 .01 .001 .01 .001 .0001                       ! Coordinate sampling.
0. 0. 0. 0. 0. 1. 'o'                             ! Reference trajectory: all initial coordinates nul, relative rigidity D=1.
1
'DRIFT'
-181.62646548
'DIPOLE'
0                                                    ! Analytical modeling of a dipole magnet.
! IL=2 here, to log trajectory coordinates in zgoubi.plt, at integration steps.
55. 2076.                                           ! Field region angle=45; reference radius set to curvature radius value.
27.5 0.49860858 0. 0. 0.                          ! Reference angle ACENT set to AT/2; Bo field at RM; indices, all zero.
60. 0.                                              ! EFB 1 with fringe field extent.
4 -.1455 2.2670 -.6395 1.1558 0. 0. 0.           ! Enge coefficients.
22.5 13. 1.E6 -1.E6 1.E6 1.E6                    ! EFB angle to ACENT; 13 deg EFB tilt angle; EFB is straight.
60. 0.                                              ! EFB 2 with fringe field extent.
4 -.1455 2.2670 -.6395 1.1558 0. 0. 0.           ! Enge coefficients.
-22.5 -8. 1.E6 -1.E6 1.E6 1.E6                   ! EFB angle to ACENT; -8 deg EFB tilt angle; EFB is straight.
0. 0.                                              ! EFB 3. Unused.
0 0. 0. 0. 0. 0. 0. 0. 0. 0. 0.
0 0. 1.E6 -1.E6 1.E6 1.E6 0. 0. 0. 0. 0.
2 1                                                 ! Degree of interpolation polynomial; flying grid sizing is step, proper for accuracy.
4 0                                                 ! Integration step size.
2 2084.5090 -0.087266462599717 2084.5090 0.087266462599717 ! Positioning of entrance and exit.
'DRIFT'
-181.62646548
'FIT'
2
3 5 0 .1                                           ! Vary DIPOLE field.
3 64 3.66 .1
2 1e-15 999
3 1 2 #End 0. 1. 0                               ! Request nul trajcory position at exit of DIPOLE.
3 1 3 #End 0. 1. 0                               ! Request nul trajcory angle at exit of DIPOLE.

'FAISCEAU'                                         ! Local particle coordinates.
'MATRIX'                                           ! Compute transport matrix, from trajectory coordinates.
1 0
'END'
```

An excerpt from *zgoubi.res*. Coordinates of the first particle (the reference trajectory) and its path length, under FAISCEAU, at OBJET on the left hand side, locally on the right hand side:

```
5 Keyword, label(s) : FAISCEAU                               IPASS= 1
                                     TRACE DU FAISCEAU
                                     (follows element # 4)
                                     11 TRAJECTOIRES
OBJET                                FAISCEAU
D      Y(cm)  T(mr)  Z(cm)  P(mr)  S(cm)  D-1  Y(cm)  T(mr)  Z(cm)  P(mr)  S(cm)
0 1  1.0000  0.000  0.000  0.000  0.000  0.0000  0.0000  -0.000  -0.000  0.000  0.000  1.630459E+03  1
```

Transport matrix of ZGS 45 degree sector with EFB wedge angles and fringe fields (an excerpt of MATRIX computation, from *zgoubi.res*). It can be checked against matrix transport expectations. The “first order symplectic conditions” are small, which is an indication of accurate numerical integration of the trajectories across DIPOLE:

```
7 Keyword, label(s) : MATRIX                               IPASS= 1
Reference, before change of frame (particle # 1 - D-1,Y,T,Z,s,time) :
0.00000000E+00 -2.19331903E-08 -2.24434360E-08 0.00000000E+00 0.00000000E+00 1.63080750E+03 6.65146963E-02

TRANSFER MATRIX ORDRE 1 (MKSA units)
0.870365      14.6806      0.00000      0.00000      0.00000      6.08068
-2.030224E-02  0.806503      0.00000      0.00000      0.00000      0.748209
0.00000      0.00000      0.827040      16.3143      0.00000      0.00000
0.00000      0.00000      -1.580329E-02  0.897394      0.00000      0.00000
0.774666      6.08004      0.00000      0.00000      1.00000      1.63006
0.00000      0.00000      0.00000      0.00000      0.00000      1.00000

DetY-1 = -0.000003451, DetZ-1 = 0.000000379
T12=0 at -18.20 m, T34=0 at -18.18 m
First order symplectic conditions (expected values = 0) :
-3.4507E-07  3.7861E-06  0.000  0.000  0.000  0.000
```

re-adjusted magnetic field and RE, RS positioning, with the respective values

$$B_0 = 0.49860858 \text{ kG} \quad \text{and} \quad RE = RS = 2084.5090 \text{ cm}$$

6860 This is the values used in the ZGS cell simulation in Tab. 20.62,

6861 (iv) and, finally, assemble this dipole and its mirror symmetric, in a cell (Fig. 9.25
6862 and Tab. 20.62). The mirror symmetric is obtained by just permuting the entrance
6863 and exit wedge angles. The cell includes a half long-drift at each end, and a short
6864 drift between the dipoles. The three have been taken equal for simplification, 3.37 m
6865 long.

Table 20.62 Simulation input data file: ZGS cell simplified model, obtained by assembling DIPOLE taken from Tab. 20.61 and its mirror symmetric (which means, permuting entrance and exit EFB tilt angles θ), and adding drift spaces. This input data file defines the ZGS cell sequence segment S_ZGS_cell to E_ZGS_cell, for possible use in INCLUDE statements in subsequent exercises. It also defines, for the same purpose, the dipoles sequence segments S_ZGS-DIP_UP to E_ZGS-DIP_UP (first dipole of the cell) and S_ZGS-DIP_DW to E_ZGS-DIP_DW (second dipole of the cell). In these possible INCLUDE statements, this file is used under the name ZGS_cell.inc

```

File ZGS_cell.INC.dat.
! ZGS. Simplified model, 8-periodic.
'MARKER' ZGSCellMATRIX_S                               ! Just for edition purposes.
'OBJET'
1.03527036749193e3                                     ! Reference Brho: 50 MeV proton.
5                                                         ! Create an ll particle set, proper for MATRIX computation.
.001 .01 .001 .01 .001 .0001                             ! Coordinate sampling.
0. 0. 0. 0. 0. 1.                                       ! Reference trajectory: all initial coordinates nul, relative rigidity D=1.
1

'MARKER' S_ZGS_cell                                     ! ZGS cell begins here.
'DRIFT' half_longDrift
337.

'MARKER' S_ZGS-DIP_UP                                   ! 1st dipole of cell begins here.
'DRIFT'
-181.62646548
'DIPOLE' DIP_UP                                         ! Analytical modeling of a dipole magnet.
2                                                         ! IL=2 here, to log trajectory coordinates in zgoubi.plt, at integration steps.
55. 2076.                                                ! Field region angle=45; reference radius set to curvature radius value.
27.5 0.49860858 0. 0. 0.                                ! Reference angle ACENT set to AT/2; Bo field at RM; indices, all zero.
60. 0.                                                    ! EFB 1 with fringe field extent.
4 .1455 2.2670 -.6395 1.1558 0. 0. 0.                 ! Enge coefficients.
22.5 13. 1.E6 -1.E6 1.E6 1.E6                          ! EFB angle to ACENT; EFB tilt angle; EFB is straight.
60. 0.                                                    ! EFB 2 with fringe field extent.
4 .1455 2.2670 -.6395 1.1558 0. 0. 0.                 ! Enge coefficients.
-22.5 -8. 1.E6 -1.E6 1.E6 1.E6                         ! EFB angle to ACENT; EFB tilt angle; EFB is straight.
0. 0. 0. 0. 0. 0. 0. 0.                               ! EFB 3. Unused.
0. 0. 1.E6 -1.E6 1.E6 1.E6 0.
2 1                                                       ! Degree of interpolation polynomial; flying grid sizing is step, proper for accuracy.
2.0                                                       ! Integration step size.
2 2084.5090 -0.087266462599717 2084.5090 0.087266462599717 ! Positioning of entrance and exit.
'DRIFT'
-181.62646548
'MARKER' E_ZGS-DIP_UP                                   ! 1st dipole of cell ends here.
'DRIFT' shortDrift
337.

'MARKER' S_ZGS-DIP_DW                                   ! 2nd dipole of cell begins here.
'DRIFT'
-181.62646548
'DIPOLE' DIP_DW                                         ! Analytical modeling of a dipole magnet.
2                                                         ! IL=2 here, to log trajectory coordinates in zgoubi.plt, at integration steps.
55. 2076.                                                ! Field region angle=45; reference radius set to curvature radius value.
27.5 0.49860858 0. 0. 0.                                ! Reference angle ACENT set to AT/2; Bo field at RM; indices, all zero.
60. 0.                                                    ! EFB 1 with fringe field extent.
4 .1455 2.2670 -.6395 1.1558 0. 0. 0.                 ! Enge coefficients.
22.5 8. 1.E6 -1.E6 1.E6 1.E6                           ! EFB angle to ACENT; EFB tilt angle; EFB is straight.
60. 0.                                                    ! EFB 2 with fringe field extent.
4 .1455 2.2670 -.6395 1.1558 0. 0. 0.                 ! Enge coefficients.
-22.5 -13. 1.E6 -1.E6 1.E6 1.E6                       ! EFB angle to ACENT; EFB tilt angle; EFB is straight.
0. 0. 0. 0. 0. 0. 0. 0.                               ! EFB 3. Unused.
0. 0. 1.E6 -1.E6 1.E6 1.E6 0.
2 1                                                       ! Degree of interpolation polynomial; flying grid sizing is step, proper for accuracy.
2.0                                                       ! Integration step size.
2 2084.5090 -0.087266462599717 2084.5090 0.087266462599717 ! Positioning of entrance and exit.
'DRIFT'
-181.62646548
'MARKER' E_ZGS-DIP_DW                                   ! 2nd dipole of cell ends here.
'DRIFT' half_longDrift
337.
'MARKER' E_ZGS_cell                                     ! ZGS cell ends here.

'FAISCEAU'                                             ! Local particle coordinates.
'TWISS'
2 1. 1.
'MARKER' ZGSCellMATRIX_E                               ! Just for edition purposes.
'END'
ZGS. Simplified model, 8-periodic.

```

An excerpt from zgoubi.res. Coordinates of the first particle (the reference trajectory) and its path length, under FAISCEAU, at OBJET on the left hand side, locally on the right hand side:

```

18 Keyword, label(s) : FAISCEAU                               IPASS= 4
                                TRACE DU FAISCEAU
                                (follows element # 4)
                                11 TRAJECTOIRES
                                OBJET
                                FAISCEAU
                                D      Y(cm)  T(mr)  Z(cm)  P(mr)  S(cm)  D-1  Y(cm)  T(mr)  Z(cm)  P(mr)  S(cm)
0 1 1.0000  0.000  0.000  0.000  0.000  0.0000  0.0000  -0.000  -0.000  0.000  0.000  4.272614E+03

```

6866 *Lattice parameters*

6867 The TWISS command down the sequence (Tab. 20.62) produces the periodic beam matrix results shown in Tab. 20.63

Table 20.63 Results obtained running the simulation input data file of Tab. 20.62, ZGS cell - an excerpt from zgoubi.res

```

13 Keyword, label(s) : TWISS                                     IPASS= 4
Reference, before change of frame (particle # 1 - D-1,Y,T,Z,s,time) :
0.00000000E+00 -1.59240732E-05 -9.81570020E-07 0.00000000E+00 0.00000000E+00 4.27261430E+03 4.53811009E-01

Beam matrix (beta/-alpha/-alpha/gamma) and periodic dispersion (MKSA units)
28.633680 0.000002 0.000000 0.000000 0.000000 0.000000 36.853463
0.000002 0.034924 0.000000 0.000000 0.000000 0.000000 0.000003
0.000000 0.000000 37.008846 0.000001 0.000000 0.000000 -0.000000
0.000000 0.000000 0.000001 0.027021 0.000000 0.000000 0.000000
0.000000 0.000000 0.000000 0.000000 0.000000 0.000000 0.000000
0.000000 0.000000 0.000000 0.000000 0.000000 0.000000 0.000000

          Betatron tunes (Q1 Q2 modes)
          NU_Y = 0.21235913          NU_Z = 0.19286706

          Momentum compaction :
          dL/L / dp/p = 1.4126935
(dp = 0.000000E+00  L(0) = 4.27261E+03 cm, L(0)-L(-dp) = 6.03584E-01 cm, L(0)-L(+dp) = -6.03595E-01 cm)

          Transition gamma = 8.41348710E-01

          Chromaticities :
          dNu_y / dp/p = 4.70986585E-02          dNu_z / dp/p = 4.45745634E-02

```

6868

6869 The TWISS command also produces a zgoubi.TWISS.out file which details the
6870 optical functions along the sequence (at the downstream end of the optical elements.
6871 The header of that file details the optical parameters of the structure (Tab. 20.64).

Table 20.64 An excerpt of zgoubi.TWISS.out file resulting from the execution of the ZGS cell simulation input data file of Tab. 20.62. Note that the ring (4-period) wave numbers are 4 times the cell values Q1, Q2 displayed here. Optical functions (betatron function and derivative, orbit, phase advance, etc.) along the optical sequence are listed as part of zgoubi.TWISS.out following the header. The top part and last line of that listing are given below

```

@ LENGTH           %le  42.72614305
@ ALFA             %le  1.412693458
@ ORBIT5          %le  -0
@ GAMMATR         %le  0.8413487096
@ Q1               %le  0.2123591260 [fractional]
@ Q2               %le  0.1928670550 [fractional]
@ DQ1             %le  0.4709865847E-01
@ DQ2             %le  0.4457456345E-01
@ DXMAX           %le  3.81566835E+01 @ DXMIN           %le  3.68534544E+01
@ Dymax           %le  0.00000000E+00 @ DYMIN           %le  0.00000000E+00
@ XCOMAX          %le  3.68530296E-01 @ XCOMIN          %le  -1.59240732E-07
@ YCOMAX          %le  0.00000000E+00 @ YCOMIN          %le  0.00000000E+00
@ BETYMAX         %le  3.25272034E+01 @ BETYMIN         %le  2.86307346E+01
@ BETYMIN         %le  3.73198843E+01 @ BETYMIN         %le  3.50936471E+01
@ XCORMS          %le  8.67153286E-04
@ YCORMS          %le  0.
@ DXRMS           %le  6.22665688E-01
@ DYRMS           %le  0.00000000E+00

```

Top and bottom four lines (truncated) of zgoubi.TWISS.out optical functions listing, including the periodic β_x , β_y (β_Y , β_Z in zgoubi notations) and D_x (η_Y in zgoubi notations) values at cell ends:

```

# alfx      btx      alfy      bty      alfl      btl      Dx      Dxp      etc.
-2.2668087e-6  2.8636996e+1 -1.0203802e-6  3.7013045e+1  0.0000000e+0  0.0000000e+0  3.6856253e+1  1.2733594e-4  etc.
-2.2589191e-6  2.8636995e+1 -9.9937511e-7  3.7013042e+1  0.0000000e+0  0.0000000e+0  3.6853463e+1  2.6012859e-6  etc.
-2.2589191e-6  2.8636995e+1 -9.9937511e-7  3.7013042e+1  0.0000000e+0  0.0000000e+0  3.6853463e+1  2.6012859e-6  etc.
-1.1768220e-1  2.9033592e+1 -9.1049986e-2  3.7319884e+1  0.0000000e+0  0.0000000e+0  3.6853472e+1  2.6012859e-6  etc.
.....
1.1775697e-1  2.9027748e+1  9.1140989e-2  3.7313084e+1  0.0000000e+0  0.0000000e+0  3.6853454e+1  2.6012859e-6  etc.
1.1775697e-1  2.9027748e+1  9.1140989e-2  3.7313084e+1  0.0000000e+0  0.0000000e+0  3.6853454e+1  2.6012859e-6  etc.
5.1297527e-5  2.8630735e+1  7.3912348e-5  3.7005690e+1  0.0000000e+0  0.0000000e+0  3.6853463e+1  2.6012859e-6  etc.
5.1297527e-5  2.8630735e+1  7.3912348e-5  3.7005690e+1  0.0000000e+0  0.0000000e+0  3.6853463e+1  2.6012859e-6  etc.

```

6872 (b) Betatron functions of the ZGS cell.

6873 Among the various ways to produce the betatron functions along the sequence
6874 (and throughout the DIPOLES), here are two possibilities, based on the storage of
6875 particle coordinates in zgoubi.plt during stepwise raytracing:

- 6876 1. a direct way consists in using OBJET[KOBJ=5] and transport the 11-particle set
6877 so obtained across the sequence. Then, betaFromPlt from zgoubi toolbox [2] can
6878 be used to compute the transport matrix, step by step across the sequence, from
6879 the coordinate values logged in zgoubi.plt during the stepwise integration;
- 6880 2. an indirect way consists in launching a few particles on a common invariant (hor-
6881 izontal and/or vertical) and subsequently plot the s-dependent quantities $\hat{Y}^2(s)/\epsilon_Y$
6882 and/or $\hat{Z}^2(s)/\epsilon_Z$. The maximum value of the latter, a function of the distance s,
6883 is the betatron function along the sequence, $\beta_{Y,Z}(s)$.

6884 The second method is used here (this is an arbitrary choice. Exercises may be
6885 found in the various Chapters, that use the first method and may be referred to, if
6886 desired).

The input data file to derive the betatron function following method (2) above is given in Tab. 20.65. The initial ellipse parameters (under OBJET) are the periodic values, namely, $\alpha_Y = \alpha_Z = 0$, $\beta_Y = 28.63$ m, $\beta_Z = 37.01$ m, they are a sub-product of the TWISS procedure performed in (a), to be found in zgoubi.TWISS.out (Tab. 20.64). The resulting envelopes and their squared value are shown in Fig. 20.72. Note that this raytracing also provides the coordinates of the 60 particles on their common upright invariant

$$x^2/\beta_x + \beta_x x'^2 = \epsilon_x/\pi$$

6887 at start and at the end of the cell (with x standing for either Y or Z, and $\epsilon_{Y,Z}/\pi =$
6888 10^{-4} , here). This allows checking that the initial ellipse parameters (under OBJET,
6889 Tab. 20.65) are effectively periodic values, and that the raytracing went correctly,
6890 namely by observing that the initial and final ellipses do superimpose (Fig. 20.73).

Table 20.65 Simulation input data file: raytrace 60 particles across ZGS cell to generate beam envelopes. Store particle data in zgoubi.plt, along DRIFTS and DIPOLES. The INCLUDE file and segments are defined in Tab. 20.62

```

ZGS envelopes.
'OBJET'
1.03527036749193e3                               ! Reference Brho: 50 MeV proton.
8                               ! Create a set of 60 particles evenly distributed on the same invariant;
1 60 1 ! case of 60 particles on a vertical invariant; use 60 1 1 instead for horizontal invariant.
0. 0. 0. 0. 0. 1.
0. 2.8637014E+1 0e-4
0. 3.7012633E+1 1e-4
0. 1. 0.

'FAISTORE'                               ! This logs the coordinates of the particle to zgoubi.fai,
zgoubi.fai  S_ZGS_cell  E_ZGS_cell        ! at the two LABELIs as indicated.
1

'MARKER'  S_ZGS_cell
'DRIFT' half_longDrift                    ! Option 'split' divides the drift in 10 pieces,
337. split 10 2                          ! 'IL=2' causes log of particle data to zgoubi.plt.

'INCLUDE'
1
./ZGS_cell.inc[S_ZGS-DIP_UP:E_ZGS-DIP_UP]

'DRIFT' shortDrift
337. split 10 2

'INCLUDE'
1
./ZGS_cell.inc[S_ZGS-DIP_DW:E_ZGS-DIP_DW]

'DRIFT' half_longDrift
337. split 10 2
'MARKER'  E_ZGS_cell

'FAISCEAU'
'END'

```

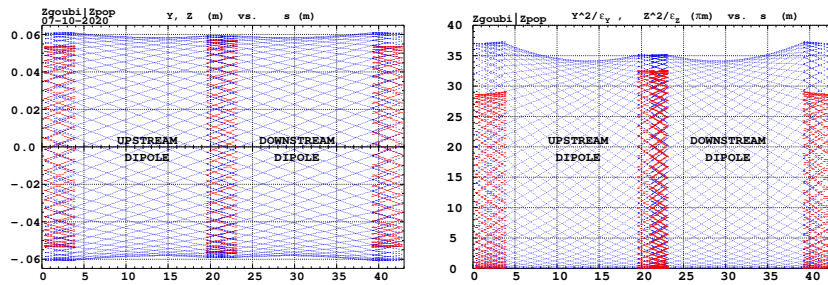


Fig. 20.72 Left: horizontal and vertical envelopes as generated by plotting the coordinates $Y(s)$ (thick lines, red, along the drifts only) or $Z(s)$ (thin lines, blue) across the ZGS cell, of 60 particles evenly distributed on a common $10^{-4} \pi \mu\text{m}$ invariant, either horizontal or vertical (while the other invariant is zero). Right: a plot of $Y^2(s)/\epsilon_Y$ and $Z^2(s)/\epsilon_Z$: the extrema identify with $\beta_Y(s)$ and $\beta_Z(s)$, respectively. The extrema extremorum values are $\hat{\beta}_Y = 32.5 \text{ m}$ and $\hat{\beta}_Z = 37.1 \text{ m}$, respectively. These plots are obtained using zpop, which reads stepwise particle data from zgoubi.plt

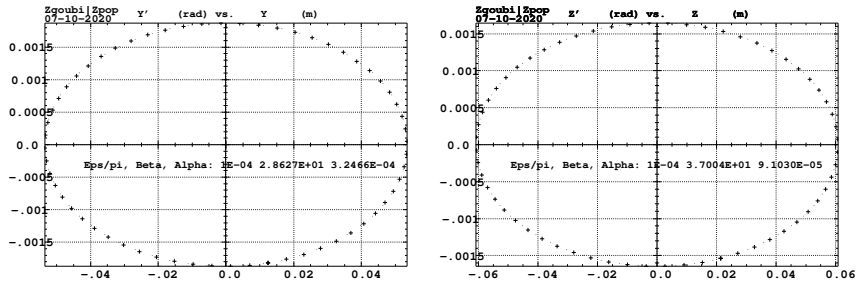


Fig. 20.73 Sixty particles evenly distributed on a common periodic invariant (of value either $\epsilon_Y = 10^{-4} \pi \mu\text{m}$ and $\epsilon_Z = 0$, left plot, or the reverse, right plot) have been tracked from start to end of the cell. These periodic invariants are defined assuming the periodic ellipse parameters determined from prior TWISS, given in Tab. 20.64; values resulting from an *rms* match of the coordinates are given in the figure, and do agree with those TWISS data. The figure shows the good superposition of the start and end invariants (the start and end *rms* match ellipse parameters show negligible difference), which confirms the correct value of the periodic ellipse parameters, namely, left graph: horizontal phase space at start (crosses) and end (dots) of the cell; right graph: vertical phase space at start (crosses) and end (dots) of the cell

6891 *Dispersion function*

6892 Raytracing off-momentum particles on their chromatic closed orbit provides the
 6893 periodic dispersion function. In order to do so, the input data file of Tab. 20.65 can
 6894 be used, it just requires changing OBJET to the following:

```
6895 'OBJET'
6896 1.03527036749193e3 ! Reference Brho: 50 MeV proton.
6897 2 ! Create particles individually'
6898 3 1 ! three particles.
6899 +36.85e-1 0. 0. 0. 1.001 'p' ! Chromatic orbit coordinates Y0 and T0 for D=1.001 relative rigidity.
6900 0. 0. 0. 0. 1. 'o' ! On-momentum orbit.
6901 -36.85e-1 0. 0. 0. 0.999 'm' ! Chromatic orbit coordinates Y0 and T0 for D=0.999 relative rigidity.
6902 1 1 1
```

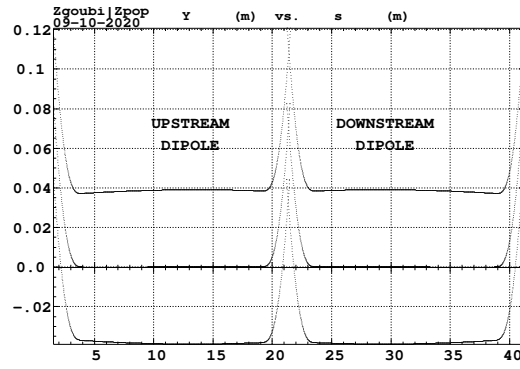
6903 The position and angle of the chromatic particles, which are offset by $\Delta p/p =$
 6904 $\pm 10^{-3}$, are drawn from the value of the periodic dispersion $\eta_Y = 36.85$ m and its
 6905 derivative $\eta'_Y \approx 0$ (Tab. 20.64), namely, $Y_0 = \eta_Y \Delta p/p = \pm 3.685$ cm and $T_0 =$
 6906 $\eta_Y \Delta p/p = 0$.

6907 Running Tab. 20.65 simulation file with this new OBJET produces the following
 6908 coordinates at FAISCEAU, located at the end of the sequence (an excerpt from
 6909 zgoubi.res):

```
6910 18 Keyword, label(s) : FAISCEAU IPASS= 1
6911 TRACE DU FAISCEAU
6912 (follows element # 17)
6913 3 TRAJECTOIRES
6914 OBJET FAISCEAU
6915 D Y(cm) T(mr) Z(cm) P(mr) S(cm) D-1 Y(cm) T(mr) Z(cm) P(mr) S(cm)
6916 p 1 1.0010 3.685 0.000 0.000 0.000 0.0000 0.0010 3.685 0.000 0.000 0.000 4.278650E+03
6917 o 1 1.0000 0.000 0.000 0.000 0.000 0.0000 0.0000 0.000 0.000 0.000 0.000 4.272614E+03
6918 m 1 0.9990 -3.685 0.000 0.000 0.000 0.0000 -0.0010 -3.685 -0.000 0.000 0.000 4.266579E+03
```

6919 The local coordinates Y, T (under FAISCEAU, right hand side) are equal to the
 6920 initial coordinates Y_0, T_0 (under OBJET, left hand side), to better than $5 \mu\text{m}, 0.5 \mu\text{rad}$
 6921 accuracy respectively (zgoubi.fai can be consulted for greater precision on these
 6922 values), so confirming the periodicity of these chromatic trajectories. Figure 20.74
 6923 shows the particle trajectories through the two DIPOLES. A difference between the
 6924 on- and off-momentum trajectories yields as expected a quasi-constant $\eta_Y \approx 36.8$ m
 6925 whereas $\eta'_Y \approx 0$. η_Y departs from exactly zero due to the fringe fields and to the
 6926 wedge focusing.

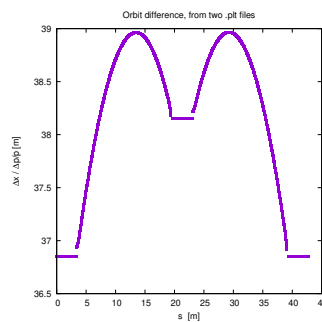
Fig. 20.74 A plot of the radial excursion, within DIPOLE range (namely, $AT=55^\circ$ extent, Tab. 20.62), of an on-momentum particle (its radial position in the dipole body is $R_0 \approx 20.7628$ m, corresponding to $Y=0$ in this graph) and two particles at respectively $dp/p = \pm 10^{-3}$. The diverging parts at DIPOLE ends are in the 5 deg fringe field regions. A graph obtained using zpop, which reads stepwise particle data from zgoubi.plt: menu 7; 1/1 to open zgoubi.plt; 2/[6,2] to select Y versus distance; 7 to plot



6927 *Orbit difference*

6928 The method can be used to compute the dispersion function, just like in machine
 6929 operation. This requires tracking a particle with $+dp/p$ momentum offset, save its
 6930 zgoubi.plt data (say, in zgoubi.plt+dpp), and repeat with $-dp/p$ (zgoubi.plt-dpp). A
 6931 gnuplot script can compute and plot the orbit difference, and normalize to dp/p ; the
 result is the periodic dispersion, displayed in Fig. 20.75.

Fig. 20.75 Dispersion function along ZGS cell, obtained by orbit difference. The discontinuities are artifacts, they are located in the overlapping regions between the optical sequence DIPOLES and DRIFTS (Tab. 20.65)



6932

6933 (c) Some verifications regarding the model.

6934 The field along large excursion orbits can be logged in zgoubi.plt, using option
6935 IL=2 (or 20, or 200, etc. for printout every 10, or 100, etc. integration step) under
6936 DIPOLE.

6937 The simulation file of Tab. 20.65 is used to raytrace five particles, with OBJET
6938 changed to the following:

```
6939 'OBJET'
6940 1.03527036749193e3 ! Reference Brho: 50 MeV proton.
6941 2 ! Create particles individually,
6942 5 1 ! five particles.
6943 +36.85e-1 0. 0. 0. 1.01 'p' ! Chromatic orbit coordinates for D=1.01 relative rigidity.
6944 0. 0. 0. 0. 1. '0' ! On-momentum closed orbit.
6945 -36.85e-1 0. 0. 0. 0.99 'm' ! Chromatic orbit coordinates for D=0.99 relative rigidity.
6946 0. 0. 5. 0. 0. 1. 'm' ! Initial vertical excursion is Z0= 5 cm off-mid-plane.
6947 0. 0. 20. 0. 0. 1. 'm' ! Initial vertical excursion is Z0=20 cm off-mid-plane.
6948 1 1 1 1 1
```

6949 Apart from the on-momentum particle (2nd in the list) this OBJET defines two
6950 particles on $\Delta p/p = \pm 1\%$ chromatic orbit (1st and 3rd in the list), this is an excursion
6951 of a few tens of centimeters, large as requested, as $\Delta x \approx 38 \times dp/p$. OBJET also
6952 defines 2 particles launched into the cell at respectively $Z_0 = 5$ cm and $Z_0 = 20$ cm.

6953 The magnetic field as a function of the azimuthal angle in DIPOLE frame, along
6954 these trajectories across the upstream DIPOLE of the cell, is shown in Fig. 20.76.
6955 The field curves for the first four trajectories essentially superimpose except for the
6956 fringe field regions (Fig. 20.76), due to the wedge angles. This behaves as expected.
6957 Detail inspection is possible, from the detailed particle coordinate and field data in
6958 zgoubi.plt - this is out of the scope of the present question.

6959 The field along the 5th particle trajectory features overshoots (Fig. 20.76), this
6960 is due to the very large vertical excursion ($Z \approx 20$ cm in the entrance fringe field
6961 region). It looks reasonable, however it may be an artifact in the case that the high
6962 order derivatives of the field in that region are large, resulting from the truncated
Taylor series method used for off mid-plane field extrapolation [1, Sec. 1.3.3].

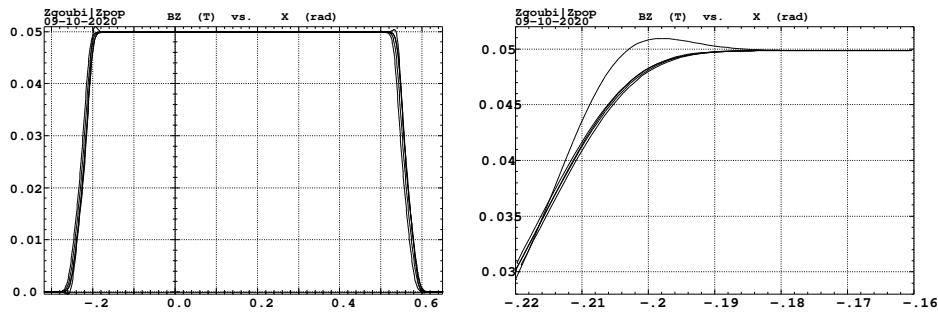


Fig. 20.76 Magnetic field along 5 different trajectories across the upstream DIPOLE, including four large horizontal and vertical excursion cases, and a zoom in on the entrance fringe field region

6964 (d) Sinusoidal approximation of the betatron motion
The approximation

$$y(\theta) = A \cos(\nu_Z \theta + \phi)$$

6965 is checked here considering the vertical motion (considering the horizontal motion
6966 leads to similar conclusions). The value of the various parameters in that expression
6967 are determined as follows:

- the particle raytraced for comparison is launched with an initial excursion $Z_0(\theta = 0) = 5$ cm (4th particle in OBJET, above). At the launch point (middle of the long drift) the beam ellipse is upright (Fig. 20.73), whereas phase space motion is clockwise, thus take

$$A = 5 \text{ cm} \quad \text{and} \quad \phi = \pi/2$$

- the vertical betatron tune of the 4-cell ring is (Tab. 20.64)

$$\nu_Z = 4 \times 0.192869 = 0.77147$$

- $\theta = s/R$ and $R = \oint ds/2\pi$ with (Tab. 20.64)

$$2\pi R = \text{circumference} = 4 \times 42.72614331 = 170.90457 \text{ m}$$

6968 The comparison with a trajectory obtained from raytracing is given in Fig. 20.77
6969 and confirms the validity of the sinusoidal approximation.

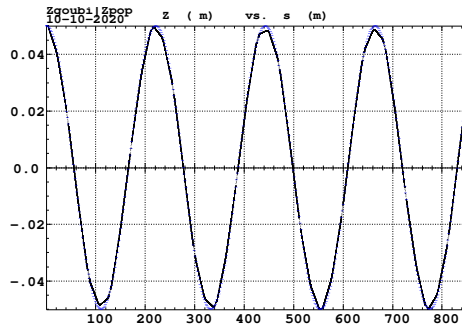


Fig. 20.77 Vertical betatron motion, five turns around the ZGS ring, from raytracing (continuous line), and sine approximation, superimposed (dashed line)

6970 (e) An acceleration cycle. Symplecticity checks.

Eleven particles are launched for 65,000 turn tracking at a rate of

$$\Delta W = q\hat{V} \cos \phi_s = 400 \times \sin 150^\circ = 200 \text{ keV/turn}$$

6971 ($E : 0.05 \rightarrow 13.05 \text{ GeV}$), all evenly distributed on the same initial vertical invariant

$$Z^2/\beta_Z + \beta_Z Z'^2 = \epsilon_Z/\pi \quad (20.17)$$

6972 with $\epsilon_Z/\pi = 10^{-4} \text{ m}$, or, normalized, $\beta\gamma\epsilon_Z/\pi = 0.33078 \times 10^{-4} \text{ m}$.

The simulation file is given in Tab. 20.66. CAVITE[IOPT=3] is used, it provides an RF phase independent boost

$$\Delta W = q\hat{V} \sin \phi_s$$

6973 as including synchrotron motion is not necessary here, even better, this ensures
 6974 constant depolarizing resonance crossing speed, so precluding any possibility of
 6975 multiple crossing (it can be referred to [3] regarding that effect).

Table 20.66 Simulation input data file: track 11 particles launched on the same vertical invariant, with quasi-zero horizontal invariant. The INCLUDE adds the ZGS cell four times, the latter is defined in Tab. 20.62 and Fig. 9.25. An MCOBJET is commented, it is used in a subsequent spin tracking exercise

```

ZGS ring. Polarization landscape.
'MARKER' ZGSPolarLand_S ! Just for edition purposes.
'OBJET'
1.03527036749193e3 ! Reference Brho: 50 MeV proton.
8 ! Create an 11 particle set, proper for MATRIX computation.
1 11 1 ! Define 9 particles, all with ~0 horiz. invarient, evenly spread on same vertical invariant.
0. 0. 0. 0. 0. 1. 'o' ! Reference trajectory: all initial coordinates nul, relative rigidity D=1.
0. 28.63 0. ! Horiz. invariant taken zero. Nominal would be 0.14mu_m norm. i.e. 4.6e-8 non-normalized.
0. 37.01 150e-6 ! epsilon_Z/pi = beta.gamma * epsilon_norm, latter =0.05e-6 m, beta.gamma=0.3308.
0. 1. 0. 0. ! All paricls are on-momentum.

!'MCOBJET' ! Commented.
!1.03527036749193e3 ! Reference Brho: 50 MeV proton.
!3 ! Create an 11 particle set, proper for MATRIX computation.
!200
!2 2 2 2 2
!0. 0. 0. 0. 0. 1.
!0. 28.63 25e-6 3 ! Periodic alpha_Y, beta_Y, and invariant value;
!0. 37.01 10e-6 3 ! Periodic alpha_Z, beta_Z, and invariant value.
!0. 1. 1.e-8 3
!123456 234567 345678

'PARTICUL'
PROTON ! Necessary data in order to allow (i) spin trackingand, and (ii) acceleration.
'SPNTRK' ! Switch on spin tracking,
3 ! all initial spins vertical.
'FAISCEAU'
'FAISTORE'
b_polarLand.fai ! Log particle data in b_polarLand.fai, turn-by-turn; "b_" imposes
7 ! binary write, which results in faster i/o.

'SCALING'
1 1
DIPOLE
-1 ! Causes field increase in DIPOLE, in correlation to particle
1. ! rigidity increase by CAVITE.
1

! 4 cells follow.
'INCLUDE'
1
4* ./ZGS_cell.inc[S_ZGS_cell:E_ZGS_cell]

'CAVITE'
3
0 0
400e3 0.523598775598 ! Acceleration rate is 400*0.5=200keV/turn.

'REBELOTE'
87000 0.3 99

'FAISCEAU'
'MARKER' ZGSPolarLand_E ! Just for edition purposes.
'SPNPRT'

'END'

```

6976 *Betatron damping*

6977 Figure 20.78 shows the damped vertical motion of the individual particles, over
 6978 the acceleration range, together with the initial and final distributions of the 11
 6979 particles on elliptical invariants. Departure from the matching ellipse at the end of
 6980 the acceleration cycle, 13 GeV (Eq. 20.17 with $\epsilon_Z/\pi = 2.2244 \times 10^{-7}$ m), is marginal.

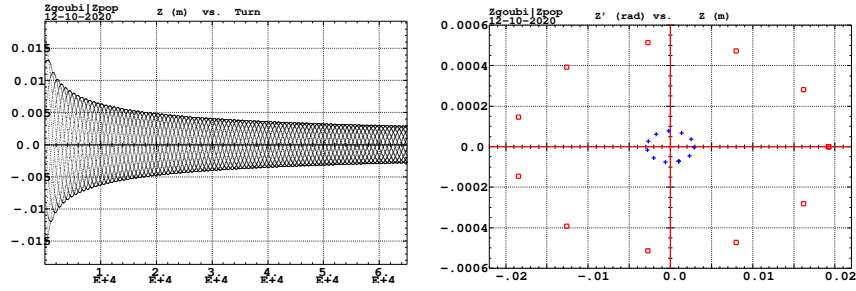
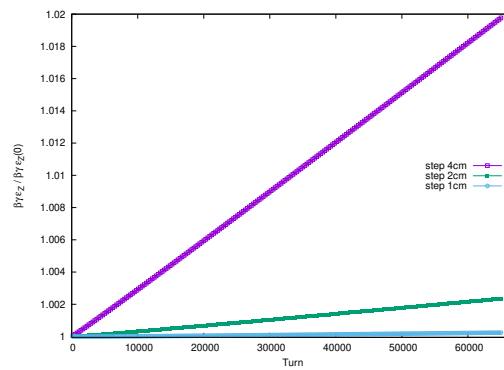


Fig. 20.78 Left: damped vertical motion, from 50 MeV to 13.05 GeV, 65,001 turns. Right: the initial coordinates of the 11 particles (squares) are taken on a common invariant $\epsilon_Z(0) = 10^{-5} \pi$ m (at 50 MeV, $\beta\gamma = 0.33078$, thus $\beta\gamma\epsilon_Z(0) = 0.33078 \times 10^{-5} \pi$ m); the final coordinates after 65,000 turns (crosses) appear to still be (with negligible departure) on a common invariant of value $\epsilon_Z(\text{final}) = 2.2244 \times 10^{-7} \pi$ m (at 13 GeV, $\beta\gamma = 14.869842$) thus $\beta\gamma\epsilon_Z(\text{final}) = 0.33076 \times 10^{-5} \pi$ m, equal to the initial value

6981 *Degree of non-symplecticity of the numerical integration*

6982 The degree of non-symplecticity as a function of integration step size is illustrated
 6983 in Fig. 20.79. The initial motion is taken paraxial, vertical motion is considered as
 6984 it resorts to off-mid plane Taylor expansion of fields [1, DIPOLE Sec.], a stringent
 6985 test as the latter is expected to deteriorate further the non-symplecticity inherent
 6986 to the Lorentz equation integration method (a truncated Taylor series method [1,
 6987 Eq. 1.2.4]).

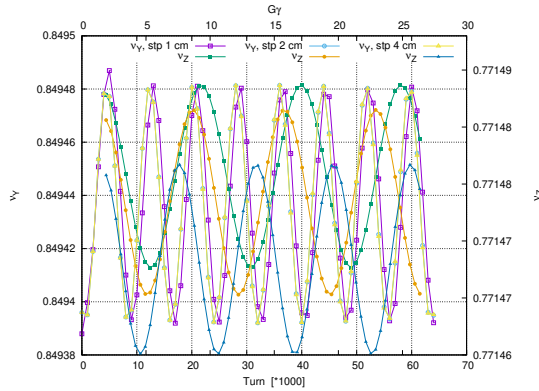
Fig. 20.79 Turn-by-turn evolution of the normalized invariant, $\beta\gamma\epsilon_z(\text{turn})/\beta\gamma\epsilon_z(0)$ (initial $\epsilon_z(0)$ taken paraxial), for four different integration step size values: 1, 2 and 4 cm



6988 *Evolution of the wave numbers.*

6989 The Fortran tool `tunesFromFai_iterate` can be used to compute tunes as a function
 6990 of turn number or energy, it reads turn by turn particle data from `zgoubi.fai` and
 6991 computes a discrete Fourier transform over so many turns (a few tens, for instance),
 6992 every so many turns [4]. Typical results are displayed in Fig. 20.80, tunes have the
 6993 expected values: $\nu_Y = 0.849$, $\nu_Z = 0.771$. An acceleration rate of 200 keV/turn has
 6994 been taken (namely, $\hat{V} = 400$ kV and still $\phi_s = 150^\circ$), to save on computing time.
 6995 Note that turn-by-turn raytracing allows determining the tune value at all γ along the
 6996 acceleration cycle (and thus for instance the γ values at which the resonance occurs,
 6997 see (f)). In these simulations anyway the horizontal and vertical tunes are essentially
 6998 constant over the all cycle: it is determined by the wedge angle, which won't change
 6999 as long as the reference orbit isn't changed. The latter holds here, as SCALING with
 7000 option NTIM=-1 causes the magnet field to strictly follow the momentum boost by
 7001 CAVITE.

Fig. 20.80 Horizontal ring tune (left vertical axis), $\nu_Y \approx 0.8494$, and vertical ring tune (right vertical axis), $\nu_Z \approx 0.77147$, as a function of turn number, over 65,000 turns ($E : 0.05 \rightarrow 13$ GeV at a rate of 200 keV/turn). The graph displays results for 3 different integration step sizes, namely, 1, 2 and 4 cm, essentially converged



7002 (f) Spin tracking. Bunch polarization.

Spin depolarizing resonances in the ZGS are located at

$$G\gamma_R = kP \pm \nu_Z = 4 - \nu_Z, 4 + \nu_Z, 8 - \nu_Z, 8 + \nu_Z, 12 - \nu_Z, \text{ etc.}$$

7003 with $P=4$ the superperiodicity of the ring, and $\nu_Z = 0.77147$ taken from Tab. 20.64,
 7004 or from Fig. 20.80. $G\gamma_R$ is bounded, in the present simulation, by $G\gamma(17.4 \text{ GeV}) =$
 7005 $35.0 < 9P - \nu_Z$. Resonances are expected to be stronger at $G\gamma_R = 2 \times 4k \pm \nu_Z =$
 7006 $8 - \nu_Z, 8 + \nu_Z, 16 - \nu_Z, \text{ etc.}$, with the additional factor 2 the number of cells per
 7007 superperiod [6, Sec. 3.II].

The simulation data file to track through these resonances is the same as in question (e), Tab. 20.66, except for the substitution of MCOBJET (to be uncommented) to OBJJET (to be commented). MCOBJET creates a 200 particle bunch with Gaussian transverse and longitudinal densities, with the following *rms* values at 50 MeV:

$$\epsilon_Y/\pi = 25 \mu\text{m}, \quad \epsilon_Z/\pi = 10 \mu\text{m}, \quad \frac{dp}{p} = 10^{-4}$$

7008 which are presumably close to ZGS polarized proton runs [7]. CAVITE accelerates
 7009 that bunch from 50 MeV to 17.4 GeV about, at a rate of $q\hat{V} \sin(\phi_s) = 200 \text{ keV/turn}$
 7010 ($\hat{V} = 400 \text{ kV}$, $\phi_s = 30^\circ$), in 87,000 turns about.

7011 Figure 20.81 shows sample S_Z spin components of a few particles taken among
 7012 the 200 tracked. Figure 20.82 displays $\langle S_Z \rangle$, the vertical polarization component of
 7013 the 200 particle set. A gnuplot script is used, given in Tab. 20.67.

Fig. 20.81 Individual vertical spin component of 20 particles accelerated in ZGS from 50 MeV to 17.4 GeV, at a rate of 200 keV/turn. This plot is obtained using zpop, which reads data from [b_]zgobui.fai: menu 7; 1/2 to open b_zgobui.fai; 2/[20,23] to select S_Z versus turn; 7 to plot

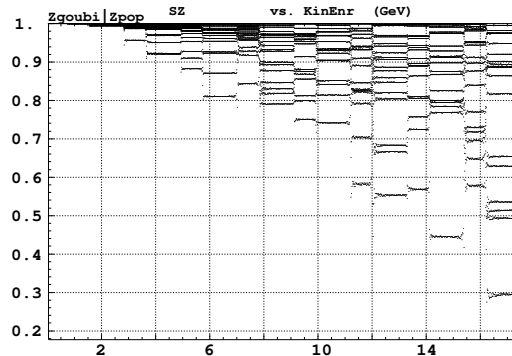


Fig. 20.82 Average vertical component of the polarization vector of a 200 particle bunch, accelerated from 50 MeV to 17.4 GeV. The vertical lines materialize the locations $G\gamma_R = 4k \pm \nu_Z$ of the depolarizing resonances. Resonances are stronger at $G\gamma_R = 8k \pm \nu_Z$ (as labeled)

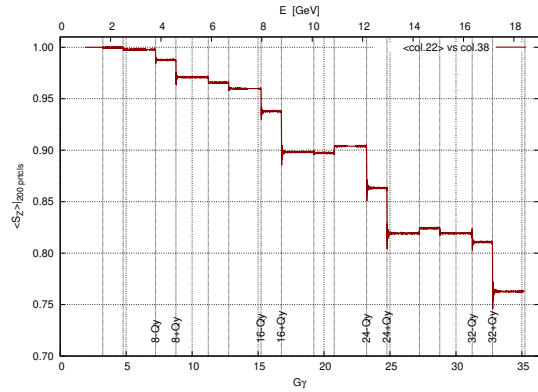


Table 20.67 A gnuplot script to plot the average vertical spin component of the 200 particle set, along the acceleration ramp (Fig. 20.82). The average is prior computed by an awk script, which reads the necessary data from zgoubi.fai.

```
# gnuplot_avgFromFai.gnu
set x2label "E [GeV]"; set xlabel "G/(Symbol g)"; set ylabel "<math>\langle S_z \rangle_{200 \text{ prtcls}}</math>"
set xtics nomirror; set x2tics; set ytics; set format y '%0.2f'; set grid
M=938.27208; Ei = 50.; G = 1.79284735; Qy = 0.7715; dE = 0.2 # MeV/turn
fName = 'zgoubi.fai'; plotCmd(col_num)=sprintf('<math>\langle S_z \rangle_{200 \text{ prtcls}}</math> vs <math>G\gamma</math>')

do for [integr=1:9] { set arrow nohead from 4*integr+Qy, 0.7 to 4*integr+Qy, 1.01 lw .6 dt 3
                    set arrow nohead from 4*integr-Qy, 0.7 to 4*integr-Qy, 1.01 lw .6 dt 3 }

do for [integr=8:32:8] { set label ".integr.-Qy" at integr-Qy, 0.71 rotate by 90
                       set label ".integr.+Qy" at integr+Qy, 0.71 rotate by 90 }

set x2r [0:19.]; set xr [0:19000./M^2G]; set yr [1:1.01]
plot plotCmd(22) u (G/M^2*(Ei+($1-1.)*dE +M)):2 w l lw 2 lc rgb 'dark-red' t "<math>\langle S_z \rangle_{200 \text{ prtcls}}</math> vs <math>G\gamma</math>"
```

average.awk script to compute $\langle S_z \rangle$ [5]:

```
function average(x, data){
  n = 0; mean = 0;
  val_min = 0; val_max = 0;
  for(val in data){
    n += 1;
    delta = val - mean;
    mean += delta/n;
    val_min = (n == 1)?val:((val < val_min)?val:val_min);
    val_max = (n == 1)?val:((val > val_max)?val:val_max);
  }
  if(n > 0){
    print x, mean, val_min, val_max;
  }
}
{
  curr = $38;
  yval = $(col_num);

  if(NR==1 || prev != curr){
    average(prev, data);
    delete data;
    prev = curr; }
  data[yval] = 1; }
END{
  average(curr, data); }
```

7014 (g) Crossing an intrinsic depolarizing resonance.

7015 The simulation data files of question (f) can be used here, Tab. 20.66, *mutatis*
7016 *mutandis*, and the methodology in (f) can be followed. In particular, the following
7017 changes are needed:

7018 • Under OBJET:

- 7019 – 1st line, change the reference rigidity *BORO* to the proper value, some distance
7020 upstream of the resonance to be crossed,
- 7021 – 3rd line, request a single particle (“1 1 1”, in lieu of “1 11 1” which distributes
7022 11 particles on the vertical invariant),
- 7023 – 6th line, set the invariant ϵ_Z/π to the desired value,
- 7024 • change the dipole field accordingly under DIPOLE, to maintains the expected
7025 curvature radius $\rho_0 = BORO/B = 20.76$ m (Tab. 9.3,
- 7026 • under CAVITE, provide the desired peak voltage \hat{V} ,
- 7027 • under REBELOTE, set the number of turns: a few thousands of turns upstream
7028 and downstream of the resonance.

7029 On the other hand, similar simulations are performed in questions (f)-(i) of
7030 exercise 9.1. Please refer to the solutions of these Saturne I simulations.

7031 (h) Study of an imperfection depolarizing resonance.

7032 The simulation data files of question (g) can be used here, *mutatis mutandis*, and
7033 the methodology in (g) can be followed.

7034 On the other hand, similar simulations are performed in questions (f)-(i) of
7035 exercise 9.1, as well as in the “Strong Focusing Synchrotron” Chapter, Sec. 20.5.
7036 Please refer to the solutions of these simulations.

7037 References

- 7038 1. Méot, F.: Zgoubi Users’ Guide.
7039 <https://www.osti.gov/biblio/1062013-zgoubi-users-guide> Sourceforge latest version:
7040 <https://sourceforge.net/p/zgoubi/code/HEAD/tree/trunk/guide/Zgoubi.pdf>
- 7041 2. A postprocessing tool to transport betatron functions step-by-step, using raytracing data stored
7042 in *zgoubi.plt*.
7043 <https://sourceforge.net/p/zgoubi/code/HEAD/tree/trunk/toolbox/betaFromPlt/>
- 7044 3. Aniel, T., et al.: Polarized particles at SATURNE. Journal de Physique, Colloque C2, supplée-
7045 ment au n02, Tome 46, février 1985, page C2-499.
7046 <https://hal.archives-ouvertes.fr/jpa-00224582>
- 7047 4. The Fortran *tunesFrmFai_iterate.f*, together with a README and an example of its use, can
7048 be found at
7049 <https://sourceforge.net/p/zgoubi/code/HEAD/tree/trunk/toolbox/tunesFromFai/>
- 7050 5. <https://stackoverflow.com/questions/42677017/plot-average-of-nth-rows-in-gnuplot>
- 7051 6. Lee, S.Y.: Spin Dynamics and Snakes in Synchrotrons. World Scientific, 1997
- 7052 7. Khoe, T.K., et al.: The High Energy Polarized Beam at the ZGS. Procs. IXth Int. Conf on
7053 High Energy Accelerators, Dubna, pp. 288-294 (1974)